Gondwana Research 128 (2024) 368–389

Contents lists available at ScienceDirect

Gondwana Research

journal homepage: www.elsevier.com/locate/gr

Record of the Indosinian Orogeny from conglomerates and detrital zircon U–Pb ages of the western Indochina Block, central Thailand

Hidetoshi Hara [a,*], Thasinee Charoentitirat [b], Tetsuya Tokiwa [c], Toshiyuki Kurihara [d], Keisuke Suzuki [d,1], Apsorn Sardsud [e]

[a] Geological Survey of Japan, National Institute of Advanced Industrial Science and Technology (AIST), 1-1-1 Higashi, Tsukuba, Ibaraki 305-8567, Japan
[b] M.Sc. in Petroleum Geoscience Program, Department of Geology, Faculty of Science, Chulalongkorn University, Bangkok 10330, Thailand
[c] Faculty of Science, Shinshu University, Matsumoto, Nagano 390-8621, Japan
[d] Graduate School of Science and Technology, Niigata University, Niigata 950-2181, Japan
[e] Department of Mineral Resources, Bangkok 10400, Thailand

ARTICLE INFO

Article history:
Received 11 April 2023
Revised 29 September 2023
Accepted 27 November 2023
Available online 30 November 2023
Handling editor: Yunpeng Dong

Keywords:
Indosinian Orogeny
Indochina Block
Unconformity
Conglomerate
U–Pb age

ABSTRACT

Middle Triassic to Early Jurassic conglomerates and associated sedimentary rocks that record the Indosinian Orogeny are exposed in the western Indochina Block, central Thailand. To elucidate the tectonic and sedimentary history of the Indosinian Orogeny, we studied the conglomerates and analyzed detrital zircon U–Pb ages of samples from the conglomerates and associated sedimentary rocks. On the basis of provenance analysis and estimation of depositional ages, the three recognized events (I, II, and III) of the Indosinian Orogeny are identified. The Indosinian I Event is represented by Type-1 limestone conglomerates, which were derived from collapse of the Permian carbonate platform. This event took place during the Norian (middle Late Triassic) and was triggered by collision between the Indochina and South China blocks. The Indosinian II Event is represented by Type-2 conglomerates, which are composed of various types of clasts, as well as basaltic sandstones. These sedimentary rocks were derived from the uplift and collapse of the Sukhothai Arc, the Nan Back-arc Basin, the Phetchabun Volcanic Belt, and basement rocks of the Indochina Block. Event II occurred as a result of the closure of the Paleo-Tethys and the commencement of collision between the Sibumasu Block, the Sukhothai Arc, and the Indochina Block during the Rhaetian (latest Triassic). The Indosinian III Event is represented by Type-3 conglomerates, which comprise volcaniclastic rocks and volcanic breccias composed of andesite and dacite. Event III occurred after the Toarcian (late Early Jurassic), associated with post-collision magmatism that occurred between the Sibumasu and Indochina blocks. Our study clarifies the timing and nature of Indosinian Orogeny I, II, and III events in the western Indochina Block and reveals that the Indosinian Orogeny involved Paleo-Tethyan subduction and micro-continental collision tectonics and associated processes during the Middle Triassic to Early Jurassic.

1. Introduction

The Indosinian Orogeny was a major event that contributed to the build-up of the Asian mainland and took place over most of southeastern to eastern Asia during the Permian to Triassic. The orogeny resulted from the amalgamation of micro-continents derived from the Gondwana margin (Carter and Clift, 2008; Arboit et al., 2016a; Metcalfe, 2021). The main stage of the Indosinian Orogeny is evidenced by Early to Late Triassic metamorphism and magmatism along the Ailaoshan–Red River and Song Ma faults (Fig. 1) and was caused by collision between the South China and Indochina blocks (Carter et al., 2001; Faure et al., 2014; Liu et al., 2015; Tran et al., 2020; Nakano et al., 2021). Liu et al. (2018) examined latest Permian to Triassic granitoids and proposed three main stages of tectonism in the Indosinian Orogeny: 1) arc magmatism and the commencement of continental collision during 255–248 Ma; 2) continental subduction during 247–237 Ma; and 3) post-collision continental exhumation during 235–202 Ma. After these events, sandstone red beds and conglomerates were overlain on the Triassic orogenic rocks with a widespread and major intervening unconformity, referred to as the Indosinian Unconformity (Lacassin et al., 1998). Investigation of Triassic marine and terrigenous sediments above and below the unconformity has allowed

* Corresponding author.
E-mail address: hara-hide@aist.go.jp (H. Hara).
[1] Present address: Geological Survey of Japan, AIST, 1-1-1 Higashi, Tsukuba, Ibaraki 305-8567, Japan.

https://doi.org/10.1016/j.gr.2023.11.009
1342-937X/

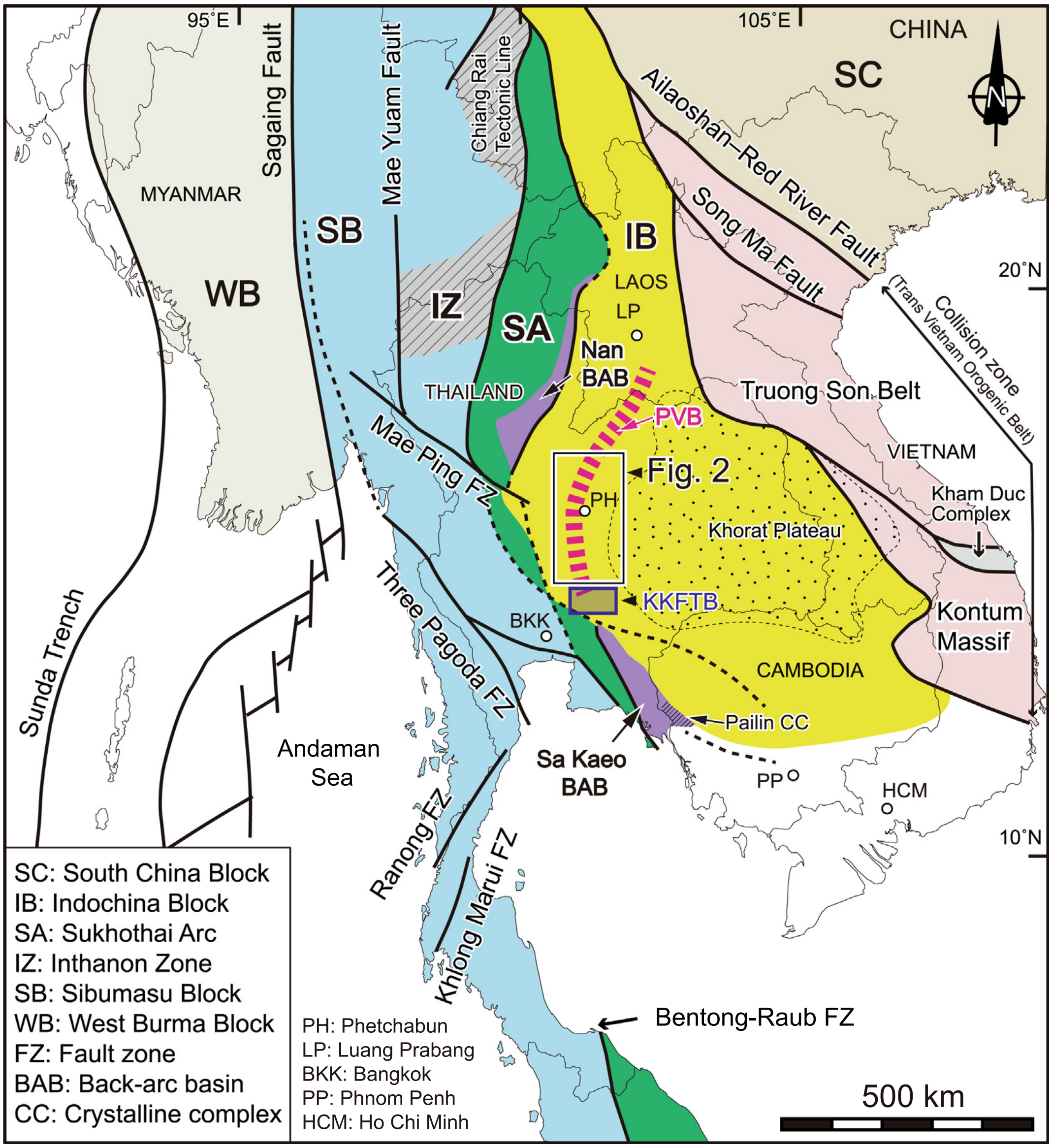

Fig. 1. Tectonic map of southeastern Asia, showing major units and fault zones (modified after Hara et al., 2021). KKFTB = Khao Khwang Fold and Thrust Belt; PVB = Phetchabun Volcanic Belt.

the depositional settings related to the Indosinian Orogeny to be reconstructed in the continental margins of the southern South China and northern Indochina blocks (Rossignol et al., 2018). Rossignol et al. (2018) concluded that both the Song Da Basin (South China Block) and the Sam Nua Basin (Indochina Block) contain a widespread and major unconformity between the Ladinian and upper Norian, representing the Indosinian Orogeny, and that both basins developed together in a terrestrial environment as a syn- to post-orogenic foreland basin after the Song Ma Ocean closure during the late Norian to the Rhaetian. Thus, the Indosinian Orogeny is recorded in metamorphic, igneous, and sedimentary rocks in and around the collision zone between the South China and Indochina blocks.

More detailed signatures of the Indosinian Orogeny have been proposed from the subsurface geology of the Khorat Plateau (Khorat Basin) in the Indochina Block (Racey et al., 1996; Booth and Sattayarak, 2011; Minezaki et al., 2019). In the Khorat Basin, the Indosinian Orogeny was characterized by three events during the Early to Middle Triassic (Event Ⅰ), Late Triassic (Event Ⅱ), and Early to Middle Jurassic (Event Ⅲ), as evidenced by marked unconformities. In addition, intensive deformation of the Permian Saraburi Group, which developed as a carbonate platform in the southwestern Indochina Block, records the tectonic history associated with the Indosinian Orogeny in the Khao Khwang Fold and Thrust Belt (KKFTB) in central Thailand (Fig. 1; Morley et al., 2013; Arboit et al., 2014, 2015). The occurrence of this tectonism in the KKFTB is supported by detrital zircon U–Pb analyses and the study of mafic and intermediate dikes in the belt (Arboit et al., 2016a, b), structural analysis of detachment faults and illite K–Ar dating of fault gouges (Hansberry et al., 2014, 2015, 2017), and U–Pb dating of calcite veins related to brittle deformation events (Simpson et al., 2021). In contrast, the geological evidence in the Triassic to Jurassic syn-tectonic sedimentary basins of the Indosinian Orogeny within the Indochina Block has not been well resolved from the surface geology. The Late Triassic Huai Hin Lat and Nam Phong formations and the Jurassic Phu Kradung Formation related to the Indosinian Orogeny are distributed in the Phetchabun–Lamnarai area of central Thailand (Fig. 2), but outcrop exposures are scattered, and continuous successions between unconformities are lacking. Geological evidence from

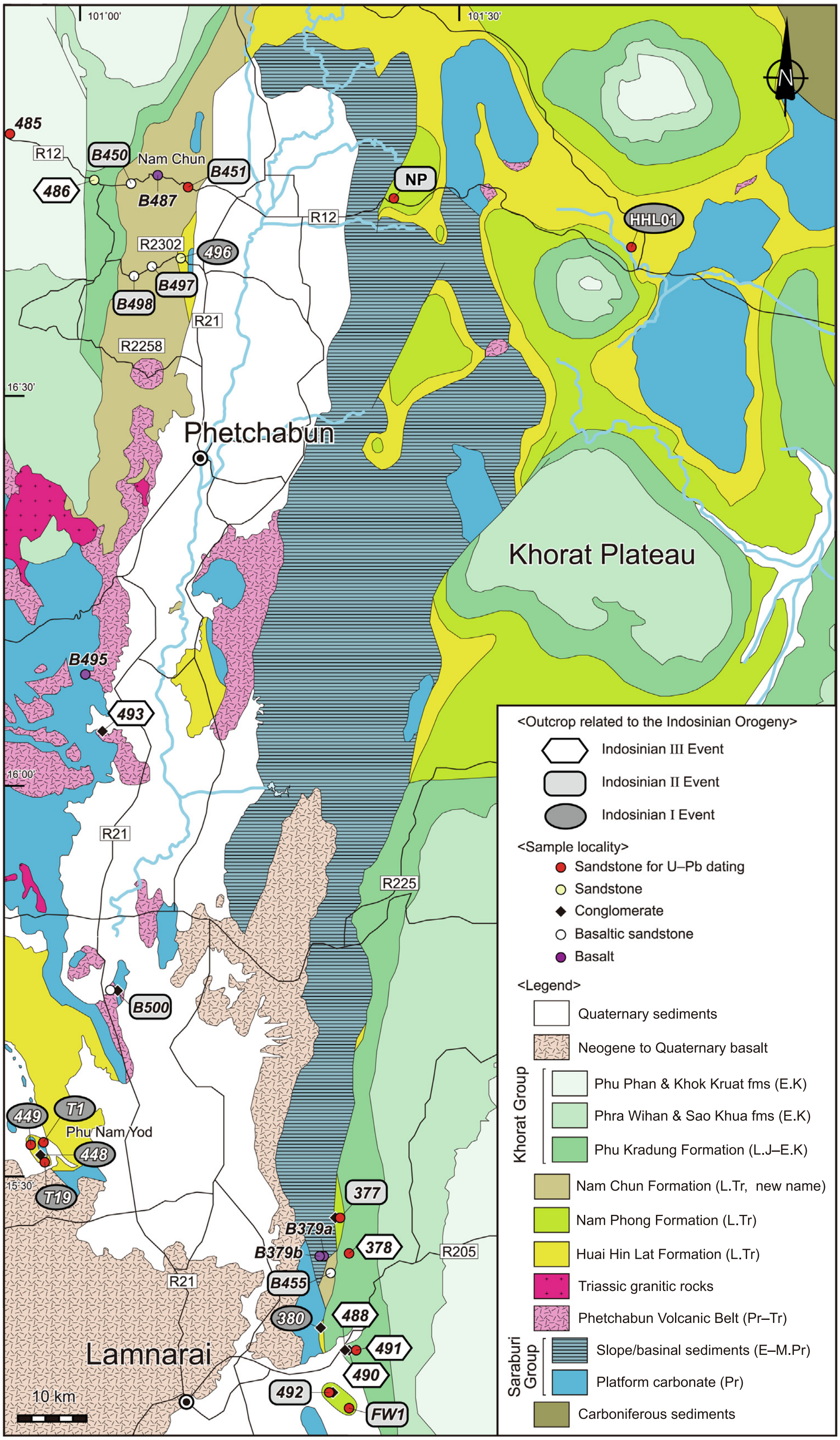

Fig. 2. Geological map of the Phetchabun–Lamnarai area in central Thailand (see Fig. 1 for location), showing sample and outcrop locations. The geological map is based on Nakornsri (1976), Chonglakmani and Satayarak (1984), Department of Mineral Resources (1999), Chairangsee and Assavapatchara (2009), Khaowiset and Chanfoo (2009), Ueno and Charoentitirat (2011), and our field survey. Pr = Permian; Tr = Triassic; J = Jurassic; K = Cretaceous; E = Early/early; M = Middle/middle; L = Late/late.

syn-tectonic sedimentary basins of the Indosinian Orogeny gained from the surface geology is less than that obtained from the subsurface geology. However, our recent field reconnaissance discovered several typical conglomerates accompanying these formations in the Phetchabun–Lamnarai area. The conglomerates provide important information about the sedimentary provenance and uplift and erosion processes during orogenesis (Aitchison et al., 2002; Wang et al., 2010; Zhang et al., 2019; Campbell et al., 2022).

The aim of this paper is to reconstruct the Indosinian Orogeny as recorded in conglomerates and associated formations in the Phetchabun–Lamnarai area in the western Indochina Block. In this study, we focus on the provenance of conglomerates and associated sedimentary rocks, as they are expected to have preserved sedimentary and erosional events related to the Indosinian Orogeny. In addition, we generate and examine detrital zircon U–Pb ages to constrain the depositional ages of the conglomerates and associated formations. These ages are also helpful in resolving the timing of Indosinian Ⅰ, Ⅱ, and Ⅲ events. Furthermore, the Indosinian Orogeny within the Indochina Block is interpreted to have been related not only to collision between the South China and Indochina blocks but also to Paleo-Tethyan subduction beneath the Indochina Block (Barber et al., 2011; Minezaki et al., 2019; Burrett et al., 2021; Morley et al., 2022). In this study, we provide new insights into Indosinian Ⅰ, Ⅱ, and Ⅲ events, based on the depositional process and age of the conglomerates overlying Indosinian Ⅰ, Ⅱ, and Ⅲ unconformities. In addition, we discuss that the triggers of Indosinian Ⅰ, Ⅱ, and Ⅲ events were associated with tectonics involving continental collision and Paleo-Tethyan subduction during the Middle Triassic to Early Jurassic within the Indochina Block.

2. Geological outline

The Paleo-Tethys convergence zone, located between the Indochina and Sibumasu blocks in southeastern Asia, was formed by subduction of Paleo-Tethyan oceanic crust beneath the present western margin of the Indochina Block (e.g., Barber et al., 2011). The Sukhothai Arc evolved within the convergence zone and was characterized by the eruption of volcanic successions, intrusion of I-type granitoids, deposition of forearc basin sediments, and the development of a back-arc basin (e.g., Hara et al., 2021). The study area is located in the western Indochina Block, including the western edge of the Khorat Plateau, behind the Sukhothai Arc, and the Nan Back-arc Basin (Fig. 1). The Permian carbonate platform with slope and basinal sedimentary rocks (the Saraburi Group; Ueno and Charoentitirat, 2011), Permian to Triassic volcanic rocks (Phetchabun Volcanic Belt; Barr and Charusiri, 2011), Late Triassic non-marine sedimentary rocks (Huai Hin Lat and Nam Phong formations; Chonglakmani, 2011), and Late Jurassic to Early Cretaceous non-marine sedimentary rocks (Khorat Group; Meesok, 2011) are exposed through the Phetchabun–Lamnarai area in the western Indochina Block (Fig. 2). Recently, the Phetchabun Volcanic Belt has been interpreted as a continental magmatic arc originated from the subduction of the Nan Back-arc Basin beneath to the Indochina Block during the Early Triassic, and collision of the Sukhothai Arc and Indochina Block during the Middle Triassic (Jiang et al., 2021; Shi et al., 2021).

Indosinian Ⅰ, Ⅱ, and Ⅲ events have been identified by the existence of three unconformities (Indosinian Ⅰ, Ⅱ, and Ⅲ unconformities) developed within the Late Triassic Huai Hin Lat and Nam Phong formations and the Jurassic Phu Kradung Formation (Booth and Sattayarak, 2011). Here, we describe each formation and its equivalents distributed in the Phetchabun–Lamnarai area of central Thailand (Fig. 2). In addition, we review and compare these formations with the subsurface geology of the Khorat Basin (Fig. 3), where the Indosinian Ⅰ, Ⅱ, and Ⅲ unconformities have been clearly identified by analysis of seismic data and drill cores.

2.1. Huai Hin Lat Formation and its equivalents

The Huai Hin Lat Formation is composed of fluvial and alluvial-fan deposits, as well as organic-rich lacustrine mudstone interbedded with volcaniclastic rocks. Fossils of plants, pollens and spores, conchostracans, and vertebrates suggest a Norian age for the formation (e.g., Chonglakmani, 2011). The Huai Hin Lat Formation corresponds to the Kuchinarai Group in the Khorat Basin based on subsurface geology defined using deep wells and cores. The Huai Hin Lat Formation and the Kuchinarai Group were deposited in an extensional environment in a series of half grabens during the Late Triassic and overlie the Indosinian Ⅰ Unconformity (Booth and Sattayarak, 2011; Minezaki et al., 2019). The Kuchinarai Group contains a mixture of terrestrial and lacustrine sedimentary rocks with interbedded volcaniclastic rocks, representing diverse depositional environments. The stratigraphic thickness of the Kuchinarai Group is estimated to range from 100 to more than 500 m.

In the study area, typical limestone conglomerates overlie the Permian Saraburi Group at the Phu Nam Yod site (Fig. 2) and are considered equivalent to the Huai Hin Lat Formation. The Saraburi Group is interpreted as a platform carbonate that developed along the western margin of the Indochina Block and corresponds to the Loei Group (Ueno and Charoentitirat, 2011). The Phu Nam Yod site is a renowned part of the Phetchabun National Geopark in central Thailand, where many fossils have been found in limestone conglomerate (Paungya et al., 2020). In the eastern part of Lamnarai (Fig. 2), the Huai Hin Lat Formation maps in a narrow area on the 1:250,000 scale geological map (Nakornsri, 1976) and is also composed of limestone conglomerates.

2.2. Nam Phong Formation

The Nam Phong Formation comprises alluvial and fluvial-fan deposits, with floodplain deposits and is composed of micaceous sandstone, conglomerate, and mudstone (Racey, 2009; Chonglakmani, 2011). This formation unconformably overlies the Huai Hin Lat Formation across the Indosinian Ⅱ Unconformity and has been dated as Rhaetian on the basis of stratigraphic relationships and fossil evidence (Chonglakmani, 2011). The Nam Phong Formation is regarded as the basal sequence of the Khorat Group (Chonglakmani, 2011). In the Khorat Basin, this formation is divided into Lower and Upper sections by the Indosinian III Unconformity based on seismic data (Booth and Sattayarak, 2011; Minezaki et al., 2019), but these two parts have not been distinguished by surface geology. The Lower Nam Phong Formation consists of interbedded claystone, siltstone, and sandstone with predominantly reddish-brown color (Booth and Sattayarak, 2011). The Upper Nam Phong Formation is characterized by fining-upward sequences consisting of thick-bedded to massive reddish-brown sandstone, with conglomerate in the central and western parts of the Khorat Basin but consists of gray to reddish-brown claystone and siltstone with minor thin-bedded sandstone in the eastern part of the basin (Booth and Sattayarak, 2011). The Lower and Upper Nam Phong Formation each have a maximum thickness of approximately 1000 m. The depositional age of the Lower Nam Phong Formation is assumed to be Rhaetian, but it has not been dated in the subsurface (Booth and Sattayarak, 2011). Racey and Goodall (2009) proposed that the depositional age of the Upper Nam Phong Formation ranges from no older than Early Jurassic (Pliensbachian) to no younger than Early Cretaceous on the basis of palynological studies and assigned it to the Late Jurassic. The large gap in depositional age between the Lower and Upper Nam Phong Formation is represented by the Indosinian

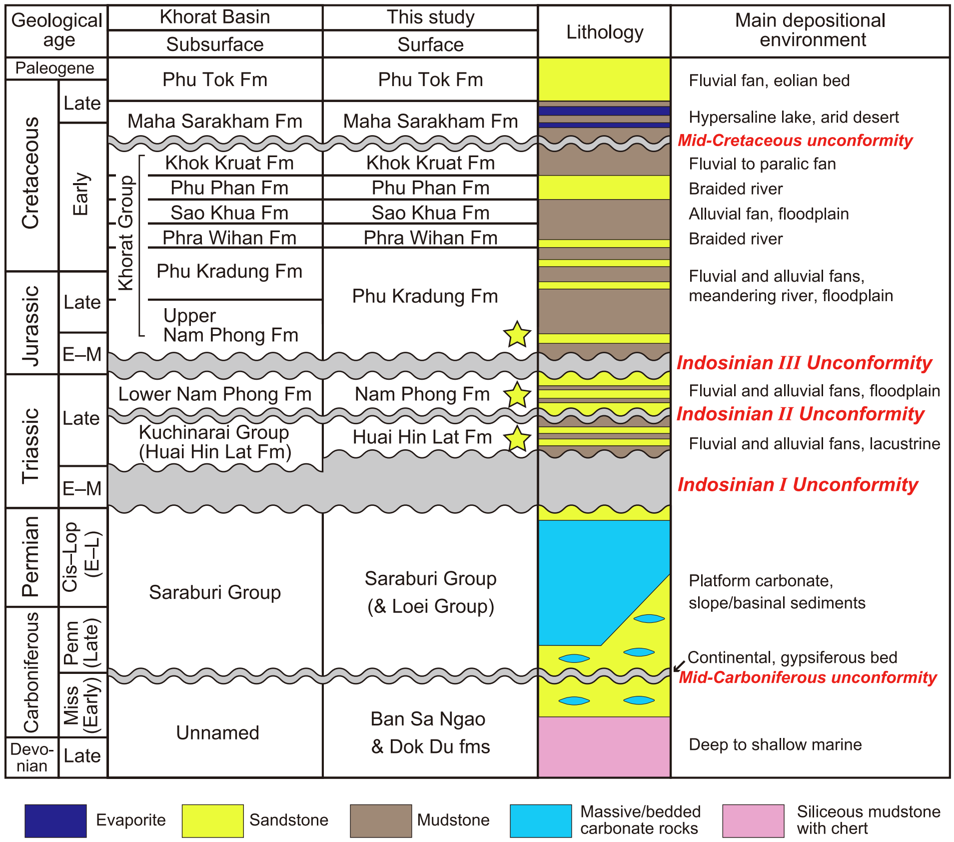

Fig. 3. Stratigraphy of the Paleozoic and Mesozoic in the Indochina Block, central to northeastern Thailand (modified after Racey, 2009; Booth and Sattayark, 2011; Ueno and Charoentitirat, 2011). Miss = Mississippian; Penn = Pennsylvanian; Cis = Cisuralian; Lop = Lopingian; E = Early/early; M = Middle/middle; L = Late/late. Star mark shows studied section.

III Unconformity. The Upper Nam Phong Formation is overlain by the Late Jurassic to Early Cretaceous Phu Kradung Formation. However, the stratigraphic relationship between these two formations is unclear, although no unconformity between them has been identified from subsurface seismic data in the Khorat Basin (Booth and Sattayarak, 2011). In addition, the Upper Nam Phong Formation have not been defined at the surface in the study area.

2.3. Phu Kradung formation

The Phu Kradung Formation of the Jurassic Khorat Group consists of a coarsening-upward sequence of sandstone, siltstone, and claystone with conglomerate (Meesok and Saengsrichan, 2011). This formation is interpreted to have been deposited in alluvial and fluvial fans and floodplain environments (Booth and Sattayarak, 2011), characterized by a meandering river system with paleosols (Horiuchi et al., 2012). The thickness of this formation is estimated to be 1400 m in the center and 500 m at the margins of the basin (Booth and Sattayarak, 2011). This formation contains both invertebrate and vertebrate faunas and floras, such as sharks, crocodilians, turtles, brachyopids, ichthyosauria, dinosaurs, and bivalves. Most of the fossil evidence suggests that this formation was deposited during the Late Jurassic (see Meesok and Saengsrichan, 2011; Cuny et al., 2014, Martin et al., 2014, Tong et al., 2014). However, palynological data from the subsurface support deposition during the Berriasian to early Barremian of the Early Cretaceous (Racey and Goodall, 2009). The depositional age of this formation is therefore estimated to be Late Jurassic to Early Cretaceous (Booth and Sattayarak, 2011), but the majority was probably deposited during the Late Jurassic.

2.4. Nam Chun Formation

The Nam Chun Formation is newly designated in this study and is distributed along the highways of Route 12 and Route 2302 in the northwestern part of Phetchabun (Fig. 2). This formation is representatively characterized by basaltic sandstone, alternating basaltic sandstone and mudstone, and basalt. On the basis of two 1:250,000scale geological maps of the Phetchabun area published by the Department of Mineral and Resources, this formation has been described as the Triassic Huai Hin Lat Formation (Chonglakmani and Satayarak, 1984) and as the Jurassic Phu Kradung Formation (Khaowiset and Chanfoo, 2009), corresponding to the different formation names presented in the earlier and recent maps. However, the characteristic lithologic sequence consisting of basaltic clastic rocks was not described in either map. Therefore, we propose the "Nam Chun Formation" for this basaltic succession, with the type locality in the Nam Chun area along Route 12. The Nam Chun Formation is assigned a depositional age equivalent to that of the Nam Phong Formation on the basis of U–Pb geochronology (described below in Section 5). Phujareanchaiwon et al. (2021) studied a continuous stratigraphic section along Route 12 that was characterized by deposits of mudstone-dominated deep-lacustrine facies and sandstone-dominated sublacustrine turbidite facies. This section is situated at Loc. B451 of this study (Fig. 2) and corresponds to the Nam Chun

Formation, although the section was assigned to the Huai Hin Lat Formation by Phujareanchaiwon et al. (2021). Outcrops with similar lithology are exposed in the eastern part of Lamnarai (Fig. 2, Loc. B455).

3. Analytical methods for geochemical analyses and zircon U–Pb dating

Twenty-one samples of clasts of volcanic rocks and ten samples of basaltic rocks were crushed in preparation for geochemical analysis. The contents of major and trace elements were determined from glass beads using X-ray fluorescence (XRF; Rigaku RIX3000) at Niigata University, Niigata, Japan. Total Fe contents are given as Fe_2O_3. Loss on ignition (LOI) was measured by weighing samples before and after 2 h of heating at 850 °C. Contents of Sc, Hf, U, and REEs for the basaltic rocks were determined using inductively coupled plasma–mass spectrometry (ICP–MS) with an Agilent 7500a instrument housed at Niigata University. Samples were prepared using a combined acid digestion procedure (HCl and HF). Analytical accuracy, as estimated by deviations from geological reference materials BHVO-2 (U.S. Geological Survey) and JB-2 (Geological Survey of Japan), was better than ± 8 %. Analytical precision, estimated from relative deviation values, was better than ± 5 %.

U–Pb dating analyses were conducted on detrital zircons selected from 10 samples of sandstone and conglomerate. Zircon grains were picked at random, mounted on glass slides, and embedded in petropoxy. Cathodoluminescence (CL) imaging was performed using a scanning electron microscope (SEM; JEOL JSM-6510) equipped with a CL system (Gatan Mini CL) at Shinshu University, Japan, to observe the internal structures and zonation patterns of zircons and to select suitable sites for U–Pb dating. For the U–Pb age determinations, U–Pb isotope abundance ratios were determined using a quadrupole-type laser-ablation (LA)–ICP–MS instrument (Agilent7700x) housed at Nagoya University, Nagoya, Japan, following the methods of Orihashi et al. (2008) and Kouchi et al. (2015). Analyses were performed with a spot size of 25 μm, a repetition rate of 10 Hz, and an energy density of 11.7 J cm^{-2}. A 213 nm solid state LA system (ESi/New Wave Research NWR213) was used for ablation. Standard zircon 91,500 with a ^{238}U–^{206}Pb age of 1062.4 ± 0.4 Ma (Wiedenbeck et al., 1995) was used for the normalization of NIST SRM 610 (Walder et al., 1993), and the latter was used as the external standard for age determinations. Accuracy was monitored through repeated analyses of the Plešovice zircon standard (Sláma et al., 2008). Ages were calculated and Concordia diagrams constructed using Isoplot v.4.15 (Ludwig, 2012). The majority of the detrital zircon U–Pb ages were concordant within 2σ analytical uncertainty. Discordant data, anomalous isotopic data, and missed-shot data of the laser beams were rejected. For this study, only concordant data were used in the calculation of detrital zircon U–Pb ages. In this paper, $^{206}Pb/^{238}U$ ages are reported for zircons with ages of < 1000 Ma and $^{207}Pb/^{206}Pb$ ages for zircons with ages of ≥ 1000 Ma.

4. Descriptions of conglomerate and basaltic sandstone

Conglomerates associated with the Indosinian Orogeny are distributed in the Phetchabun–Lamnarai area and divided into three types in this study: Type-1, Type-2, and Type-3 conglomerates. Type-1 conglomerates are attributed to the Huai Hin Lat Formation, and Type-2 and Type-3 conglomerates are attributed to the Nam Phong and Phu Kradung formations, respectively. The three types of conglomerate, basaltic sandstone, and basalt are described in this section.

In the study area, clasts within the conglomerates show weathering from both past and present processes, making the identification of clast lithology during the field survey difficult because of the strong weathering on clast surfaces and their variable color ranging from red, brown, and gray to white. In order to rock-type identification of volcanic clasts, we investigated the geochemistry of fresh clast samples using diagrams of SiO_2–(Na_2O + K_2O) (Le Bas and Streckeisen, 1991), Nb/Y–Zr/Ti (Pearce, 2008, after Winchester and Floyd, 1977), and Zr–Y (Barrett and MacLean, 1999) and compared the data with those from previous studies of volcanic rocks from the Phetchabun Volcanic Belt, the Sukhothai Arc, and post-collision tectonics (Fig. 4 and Supplementary Data 1). These volcanic rocks show a wide variation ranging from basalt to rhyolite (Fig. 4a and b) and from tholeiitic to calc-alkaline magma series (Fig. 4c). The details show that felsic volcanic rocks dominate in the Sukhothai Arc and post-collision volcanic rocks (Fig. 4a and b). On the Zr–Y diagram, the volcanic rocks of the Sukhothai Arc roughly plot in the tholeiitic to transitional field, whereas post-collision volcanic rocks plot in the calc-alkaline to transitional field (Fig. 4c). Almost data from the Phetchabun Volcanic Belt present low Zr and Y values (Fig. 4c).

4.1. Type-1 conglomerate

Limestone conglomerates are representative of the surface geology of the study area and are identified as Type-1 conglomerates in this study. The Type-1 limestone conglomerates are well exposed at the Phu Nam Yod site and in the surrounding area (Locs 448, 449, T1, and T19 in Fig. 2). Limestone clasts in the Type-1 conglomerates are usually of pebble and cobble size and are subrounded to rounded (Fig. 5a and b). The limestones have been classified as boundstone and packstone and contain abundant fossils of corals, fusulinids, gastropods, bivalves, ammonites, protozoa, trilobites, crinoid stems, sponge spicules, and ostracods (Paungya et al., 2020; Khamfoo, 2022). These fossiliferous limestones were derived from the Tak Fa Formation of the uppermost part of the Permian Saraburi Group (our unpublished data). The composition of the clasts is mainly limestone (>90 %), with minor sandstone, mudstone, and siliceous rocks. The siliceous rocks are usually black and cryptocrystalline, with SiO_2 contents of > 95 wt%, and are classified as flint occurring within limestone, not pelagic chert (Fig. 5e and Supplementary Data 1). Conglomerates are usually poorly sorted and have a red sandstone matrix. Parts of the deposits with abundant sandstone contain interbeds of conglomerate, locally showing cross-bedding at Loc. 449 (Figs. 2 and 5c). The Type-1 conglomerates with strongly weathered angular basalt pebbles are found at Loc. 380 (Fig. 5d). Geochemically, basalt pebbles plot in the fields of basalt or andesite–basaltic andesite in an Nb/Y–Zr/Ti diagram (Fig. 4b), and in the field of tholeiitic magma series (Fig. 4c). Alkaline elements (Na_2O and K_2O) were not precisely analyzed because of alteration (Fig. 4a). This conglomerate also contains pebbles of fine-grained porphyritic granite (Fig. 5f).

In the subsurface of the Khorat Basin, conglomerates of the Huai Hin Lat Formation are observed interbedded with sandstones. The clasts of the conglomerates are composed of siltstone, limestone, volcanic rock, and chert, with compositional variations between well sites (Booth and Sattayarak, 2011). The basal part of the Huai Hin Lat Formation at the Phu Wiang-1 well site contains limestone-rich conglomerates with minor igneous and sedimentary rocks, directly overlie platform carbonate deposits of the Permian Saraburi Group (Booth and Sattayarak, 2011) and are identified as Type-1 conglomerates.

4.2. Type-2 conglomerate

Type-2 conglomerates associated with the Nam Phong Formation contain clasts of varied lithology, including limestone, basalt, andesite, dacite, sandstone, and mudstone and are generally of

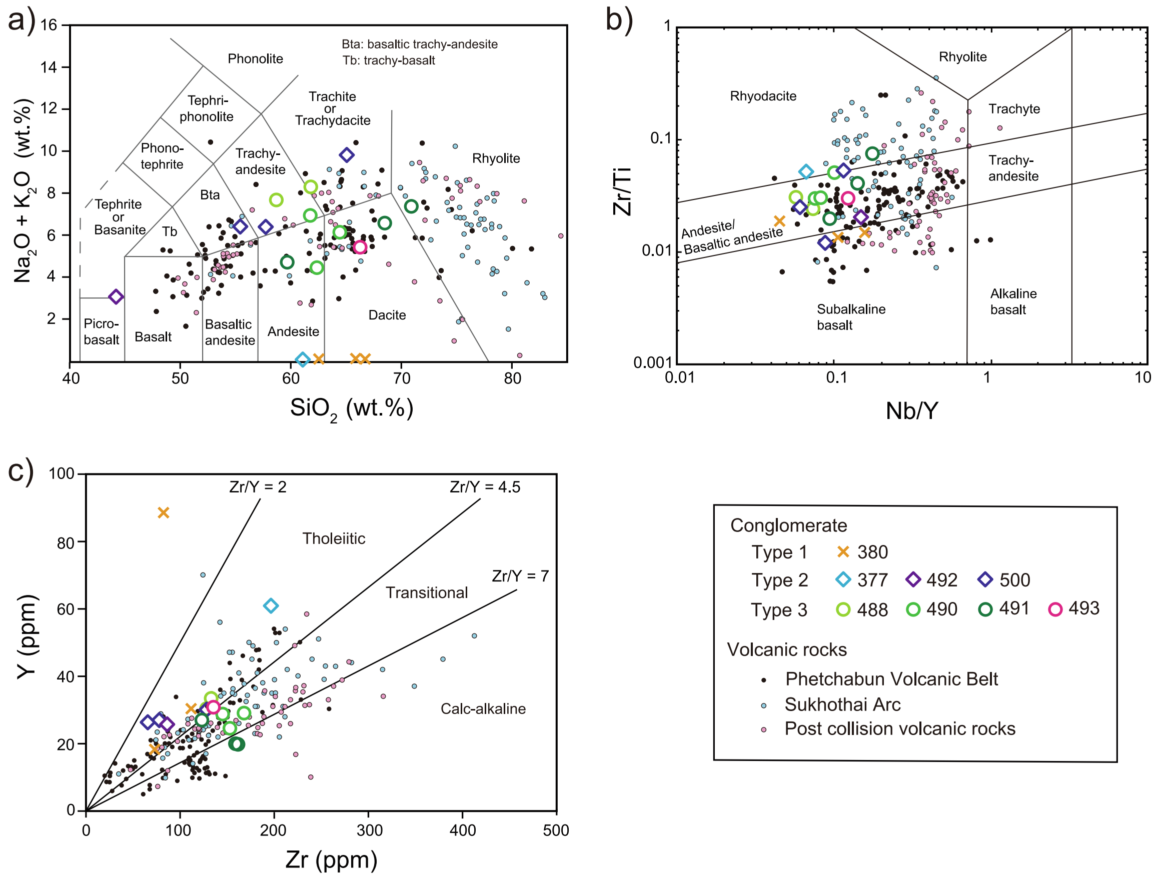

Fig. 4. Whole-rock geochemistry of volcanic rocks clasts in conglomerates. (a) SiO_2 versus $Na_2O + K_2O$ diagram (after Le Bas and Streckeisen, 1991). (b) Nb/Y versus Zr/Ti diagram (Pearce, 2008, after Winchester and Floyd, 1977). (c) Zr versus Y diagram (Barrett and MacLean, 1999). Geochemical data for the Phetchabun Volcanic Belt are compiled from Panjasawatwong et al. (2006), Boonsoong et al. (2011), Kamvong et al. (2014), Salam et al. (2014), and Qian et al. (2015); data for the Sukhothai Arc are from Barr et al. (2000, 2006) and Qian et al., (2017a); and data for post-collision volcanic rocks are from Srichan et al. (2009) and Qian et al. (2013, 2016, 2017b).

granule and pebble size. The clasts are typically subrounded, although the volcanic rock clasts are subangular. The Type-2 conglomerates are usually interbedded with reddish-brown ferruginous sandstone. At Loc. 377, the conglomerate particles are composed of various lithologies, including lithic sandstone, mudstone, basalt, andesite, dacite, and volcaniclastic rocks (Fig. 6a). The conglomerate at Loc. 492 is characterized by the occurrence of pebbles and cobbles of limestone and basalt (Fig. 6b). The basalt pebbles and cobbles are commonly altered, containing minerals such as prehnite and epidote (Fig. 6e). The conglomerate at Loc. B500 contains granules and pebbles of limestone, basalt, andesite, and dacite, and is interbedded with sandstone (Fig. 6c and d). Under microscopic observation, plagioclase phenocrysts of basalt and dacite clasts are usually fresh, whereas groundmass plagioclase is replaced by secondary calcite (Fig. 6f and g). Sandstone at Loc. B500 consists of basaltic sandstone with abundant basaltic fragments and has similar geochemical characteristics to those of basaltic sandstone of the Nam Chun Formation (described below in this section). Limestone pebbles at Loc. 492 and Loc. B500 contain scarce Permian fusulinids (our unpublished data). Geochemical characteristics suggest that the clasts composed of volcanic rocks range in composition from picro-basalt to trachyte or trachydacite (Fig. 4a), from subalkaline basalt to rhyodacite (Fig. 4b), and are classified mostly as tholeiitic magma series (Fig. 4c). These geochemical data suggest similar characteristics to data from the Phetchabun Volcanic Belt and the Sukhothai Arc.

In a previous study, Chonglakmani (2011) described conglomerates of the Nam Phong Formation in the surface as containing pebbles of quartz, brown and gray chert, and reddish-brown siltstone. However, conglomerates of the Lower Nam Phong Formation have not been identified in the subsurface of the Khorat Basin (Booth and Sattayarak, 2011). The Upper Nam Phong Formation contains conglomerate with thick-bedded to massive sandstone, with clasts in the conglomerate being composed of quartz, chert, and a variety of sedimentary, igneous, and volcanic rocks (Booth and Sattayarak, 2011). The observed lithological diversity of clasts of the Type-2 conglomerates in the surface indicates that they were sourced from various provenances.

4.3. Type-3 conglomerate

Type-3 conglomerates are observed in volcaniclastic sequences of bedded conglomerate and sandstone and are clearly exposed along a railway in eastern Lamnarai (Figs. 2 and 7a; Locs. 488, 490, and 491). The Type-3 conglomerates comprise abundant subangular to angular granules, pebbles, and cobbles composed of andesite to dacite and contain clast-supported volcaniclastic rocks and volcanic breccias (Fig. 7b). Volcaniclastic sandstones are typically interbedded with conglomerates (Fig. 7c). Type-3 conglomerates are also found at Loc. 493, where they consist of dacite and andesite granules, pebbles, and cobbles. Dacite and andesite clasts typically contain phenocrysts of plagioclase, pyroxene, and hornblende in a fine-grained groundmass (Fig. 7e), with local alteration to saussuritized plagioclase and chloritized hornblende. Geochemical data reveal that the clast compositions of volcanic rocks range from andesite, dacite to rhyolite (Fig. 4a) as well as andesite–basal-

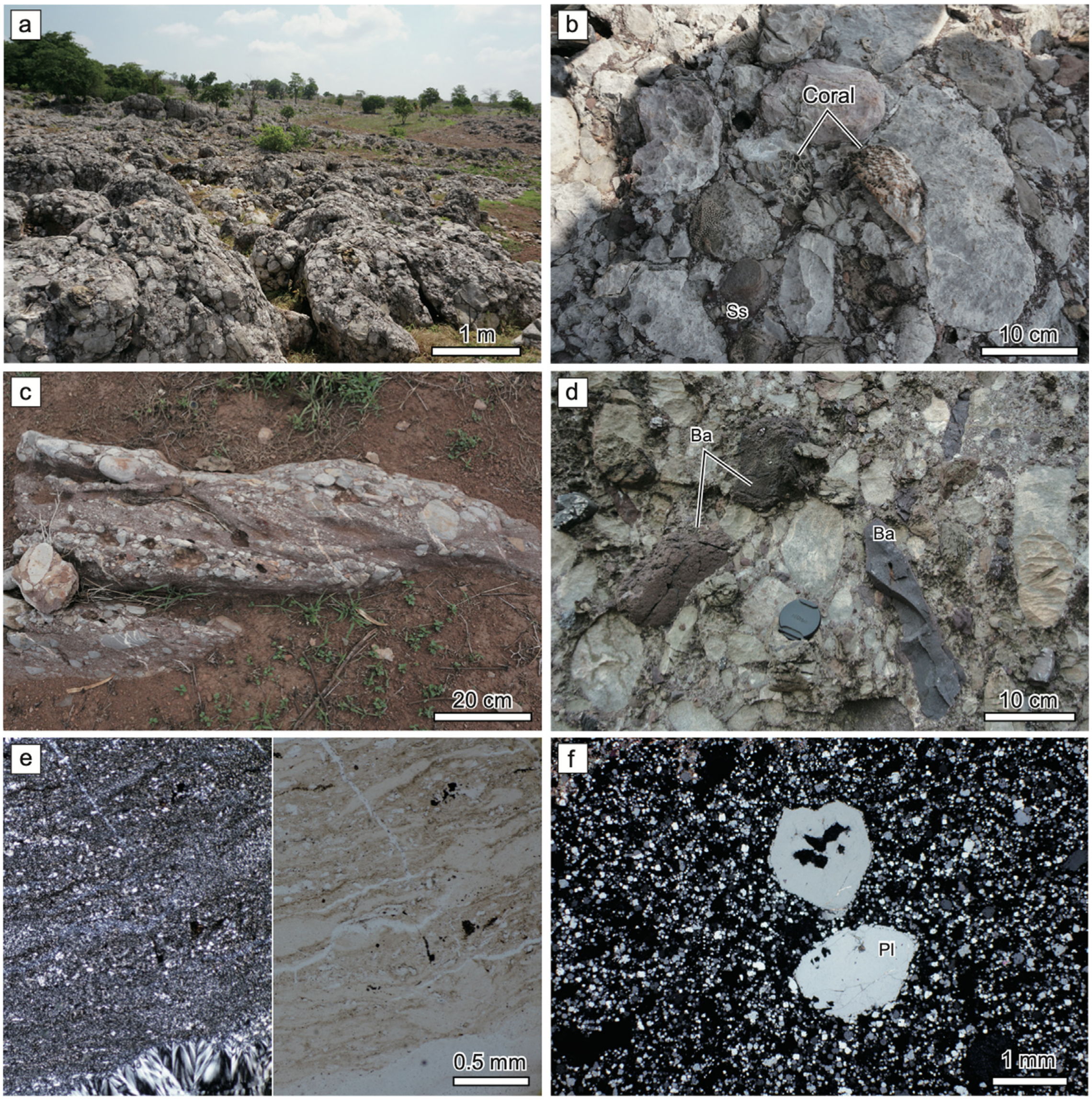

Fig. 5. Examples of the occurrence of Type-1 conglomerate. (a) Photograph of limestone conglomerate at the Phu Nam Yod site (Loc. 448). (b) Photograph of coral fossils in limestone pebbles (Loc. 448). (c) Photograph of interbedded conglomerate and sandstone showing cross-lamination (Loc. 449). (d) Photograph of limestone conglomerate with basalt pebbles (Loc. 380). (e) Photomicrograph of flint pebble (Loc. 448; left panel, plane-polarized light; right panel, cross-polarized light). (f) Photomicrograph of a pebble of fine-grained porphyritic granite with plagioclase phenocryst (Loc. 380; cross-polarized light). Ba = basalt; Pl = plagioclase; Ss = sandstone.

tic andesite to rhyodacite (Fig. 4b). In addition, geochemical data are classified mostly as calc-alkaline to transitional magma series (Fig. 4c). These trends are similar to data from the post-collision volcanic rocks, rather than the Phetchabun Volcanic Belt and Sukhothai Arc.

Volcaniclastic rocks are found at Loc. 488, where paleomagnetic and U–Pb geochronological data were obtained by Yang et al. (2019). Yang et al. (2019) proposed that this volcaniclastic conglomerate belongs to part of the volcanic sequence of the Phetchabun Volcanic Belt. However, on the basis of the geological map (Fig. 2) and detrital U–Pb ages (described below in Section 5), the volcaniclastic sequence, including Type-3 conglomerate, is designated as part of the Phu Kradung Formation in this study. Typical sandstone beds of the Phu Kradung Formation are exposed at Loc. 378 and show parallel bedding and cross-lamination (Fig. 7d). The sandstone is composed of abundant lithic fragments of volcanic rocks, quartz, and plagioclase (Fig. 7g). Type-3 conglomerate has not been identified in the subsurface of the Khorat Basin, except for thin conglomeratic channel-lag deposits in the Phu Kradung Formation (Booth and Sattayarak, 2011).

4.4. Basaltic sandstone and basalt

Basaltic sandstones are newly defined here as a member of the Nam Chun Formation. Occurrences of basaltic sandstone show stratigraphic variation between sections and between outcrops. Basaltic sandstone at Loc. B450 comprises a sequence of red siltstone and mudstone, basaltic volcaniclastic rock, and alternating basaltic sandstone and mudstone from bottom to top (Fig. 8a). The stratigraphy shows an unconformity between the basaltic volcaniclastic rock and alternating basaltic sandstone and mudstone. Interbedded basaltic sandstone and mudstone are distributed at and around Loc. B451 (Fig. 8b). This section was studied by Phujareanchaiwon et al. (2021) and is composed of deposits of mudstone-dominated deep-lacustrine facies and sandstone-dominated sublacustrine turbidite facies. At Loc. B455, cherts are

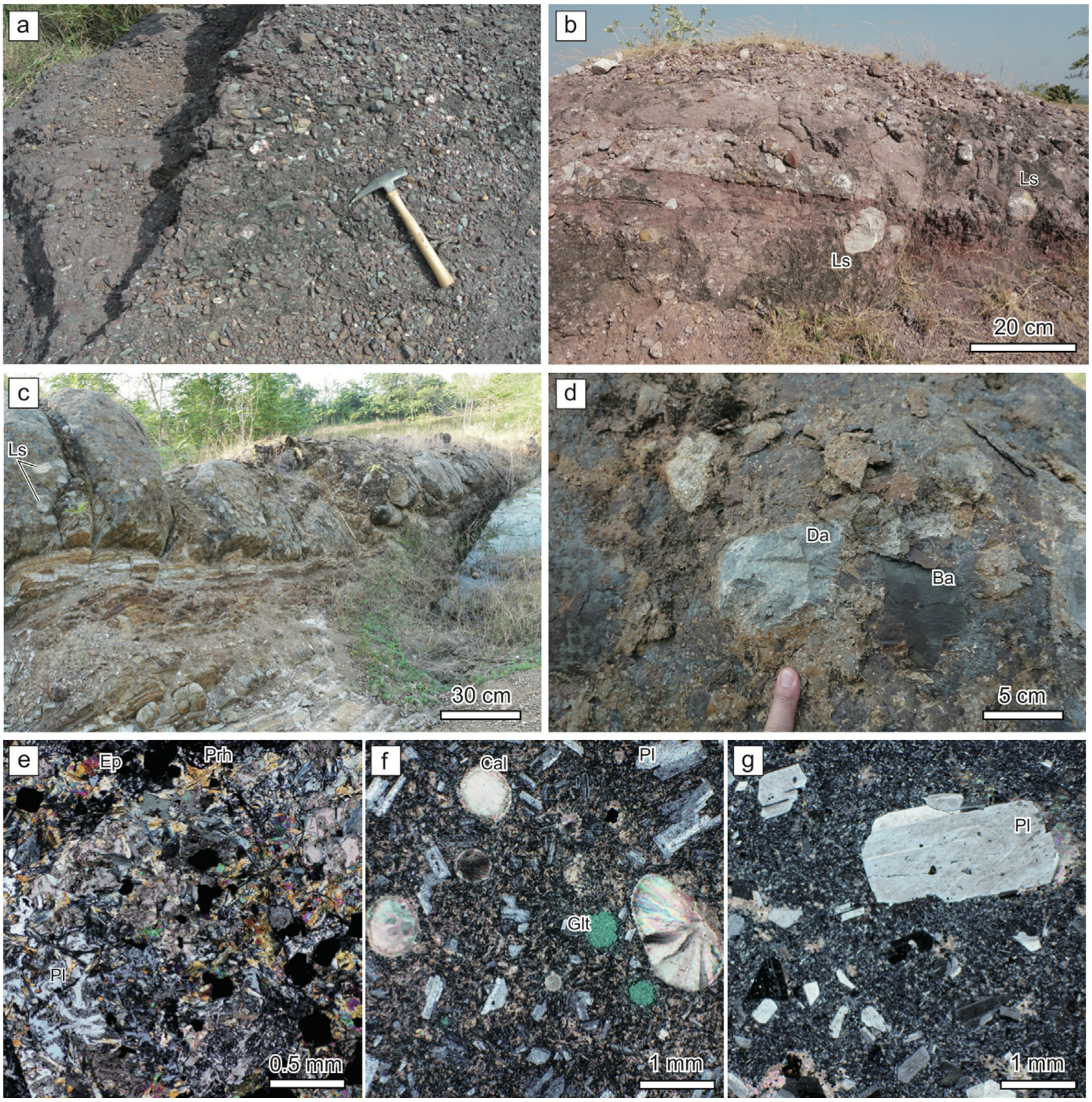

Fig. 6. Examples of the occurrence of Type-2 conglomerate. (a) Photograph of conglomerate with abundant sandstone granules and pebbles (Loc. 377). (b) Photograph of interbedded conglomerate and sandstone (Loc. 492). (c) Photograph of interbedded conglomerate and sandstone (Loc. B500). (d) Photograph of pebbles of basalt and dacite (Loc. B500). (e) Photomicrograph of altered basalt pebble with epidote and prehnite (Loc. 492). (f) Photomicrograph of basalt pebble with glauconite and amygdule replaced by calcite (Loc. B500). (g) Photomicrograph of dacite clast (Loc. B500). Photomicrographs (e)–(g) taken under cross-polarized light. Ba = basalt; Da = dacite; Ls = limestone; Cal = calcite; Ep = epidote; Glt = glauconite; Pl = plagioclase; Prh = prehnite.

interbedded with basaltic sandstone and basaltic siltstone (Fig. 8c and d). As mentioned above, the basaltic sandstones are interbedded with Type-2 conglomerate at Loc. B500. Under microscopic observation, the basaltic sandstones are composed mainly of basalt fragments, plagioclase, and clinopyroxene, with minor quartz (Fig. 8e and f). Thin basaltic siltstones are locally interbedded with the basaltic sandstones (Fig. 8g). Similar basaltic sandstones are distributed in basin-fill sediments from the Sa Kaeo Back-arc Basin (Hara et al., 2018).

Geochemically, the basaltic sandstones plot around basalt–andesite on the V–Cr–Th*10 ternary diagram (Hara et al., 2018) and around basalt on the La–Th–Sc diagram (Bhatia and Crook, 1986), suggesting direct supply from basalt (Fig. 9 and Supplementary Data 2). Basaltic sandstones in the study area are characterized by a greater abundance of basaltic fragments compared with basin-fill sediments from the Nan and Sa Kaeo Back-arc basins (Hara et al., 2018, 2021).

In addition, minor basalts and dolerites are exposed near the basaltic sandstones in this area. The basalts typically occur as massive or bedded lavas (Fig. 8h) and contain plagioclase and clinopyroxene phenocrysts in the groundmass. Euhedral plagioclase and clinopyroxene indicate porphyritic textures frequently (Fig. 8i and j). Geochemical data suggest similar characteristics between the basalts and the basaltic sandstones (Fig. 10 and Supplementary Data 2). The basaltic sandstones and basalts plot in the basalt to andesite fields on the SiO_2 – (Na_2O + K_2O) diagram (Fig. 10a; Le Bas and Streckeisen, 1991). Plots of C1-chondrite-normalized rare earth element (REE) patterns of the basaltic sandstones and basalts are flat (Fig. 10b), displaying characteristics of N-MORB (N-type mid-ocean ridge basalt). Three discrimination diagrams were used to identify the tectonic setting of the basaltic sandstones and basalts. On the Ti–V diagram (Shervais, 1982), the basaltic sandstones and basalts are scattered within the MORB and back-arc basin basalt (BABB) fields (Fig. 10c). On the ternary 2Nb–Zr/4–Y

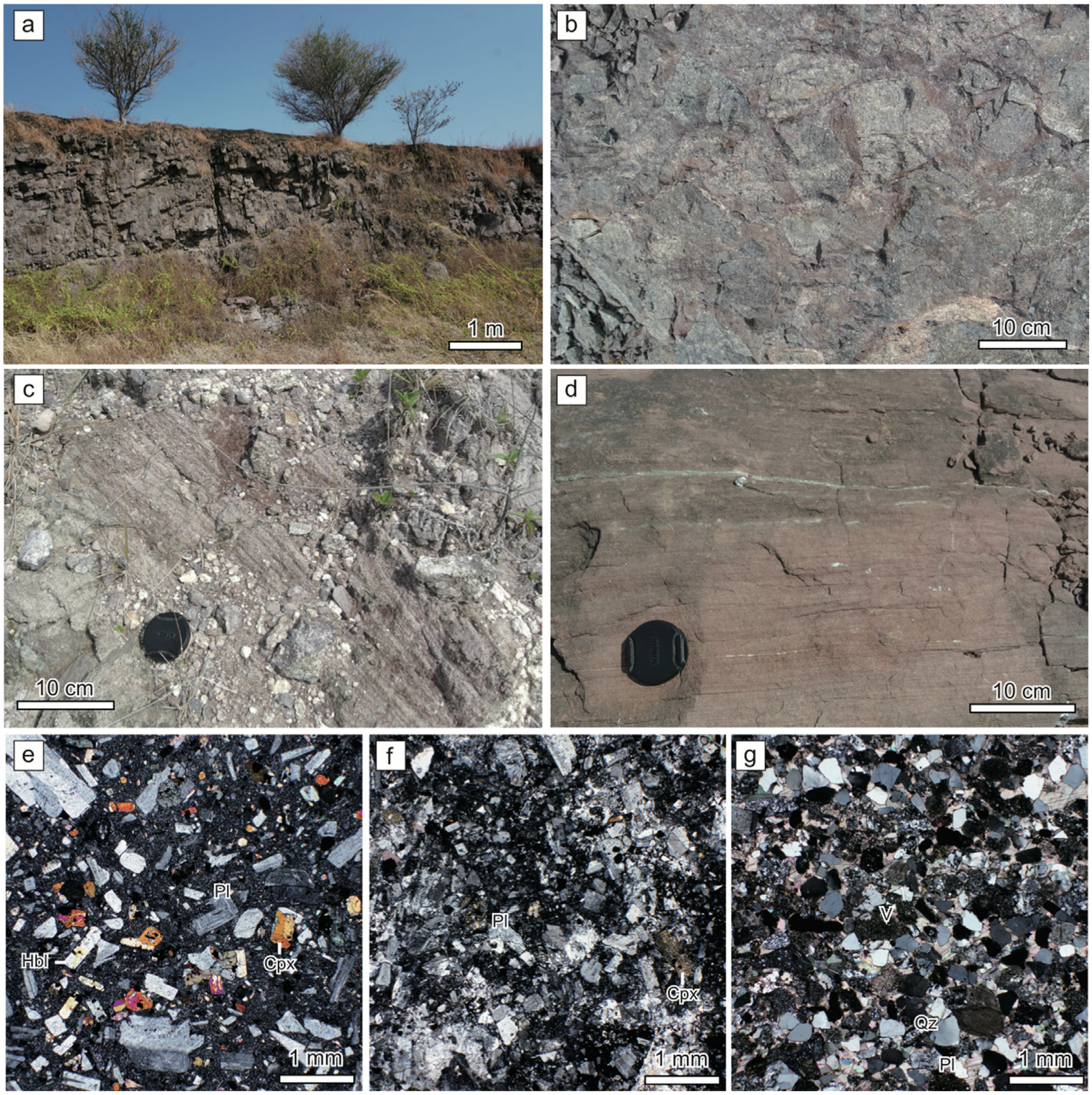

Fig. 7. Examples of the occurrence of Type-3 conglomerate. (a) Photograph of an outcrop of conglomerate (Loc. 488). (b) Photograph of volcanic breccia of andesite and dacite (Loc. 491). (c) Photograph of sandstone within conglomerate (Loc. 491). (d) Photograph of laminated sandstone (Loc. 378). (e) Photomicrograph of fresh andesite pebble (Loc. 488). (f) Photomicrograph of altered dacite pebble. (g) Photomicrograph of sandstone (Loc. 491). Cpx = clinopyroxene; Hbl = hornblende; Pl = plagioclase; Qz = quartz; V = Lithic fragment of volcanic rocks. Photomicrographs (e)–(g) taken under cross-polarized light.

diagram (Meschede, 1986), the basaltic sandstones and basalts plot in the N-MORB field (Fig. 10d). On the Nb/Yb–Th/Yb diagram (Pearce, 2008), the basaltic sandstones and basalts plot with higher Th/Yb ratios than those of the MORB–ocean island basalt (OIB) array (Fig. 10e). A comparison between our new and available published data from the Nan and the Sa Kaeo Back-arc basins and the Pailin Crystalline Complex (Macdonald and Barr, 1984; Barr and Macdonald, 1987; Hara et al., 2018, 2020) reveals that the basaltic sandstones and basalts have similar geochemical characteristics to those of some Nan Back-arc Basin basalts, Type-1 basalt of the Sa Kaeo Back-arc Basin, and amphibolite of the Pailin Crystalline Complex (Fig. 10b–e). The geochemical evidence suggests that back-arc basin basalts were widely exposed in the study area, although most of the basalts have been covered by younger sediments since their eruption, and that the basaltic sandstones were derived from these back-arc basin basalts.

5. Detrital zircon U–Pb ages of sandstones and conglomerates

Detrital zircon U–Pb ages of sandstones were determined to constrain the depositional age and provenance of each formation associated with the Indosinian Orogeny. U–Pb dating was conducted on zircons from 10 samples using LA–ICP–MS. The youngest zircon U–Pb ages were used to constrain the maximum depositional age of each sample: the youngest single-grain (YSG) zircon age, and the weighted mean age of the youngest cluster (YC) that overlaps within 1σ uncertainty (Hara et al., 2021). The ages were calculated and concordia diagrams constructed with IsoPlot v.4.15 (Ludwig, 2012) and Isoplot R (Vermeesch, 2018). In addition, the "unmix age" function of IsoPlot v.4.15 (Ludwig, 2012) and the "mixture model" function of DensityPlotter (Vermeesch, 2012) were applied to samples 377, 449, 492, T1, and FW1, which have multiple peaks in the youngest U–Pb age cluster. These estimated

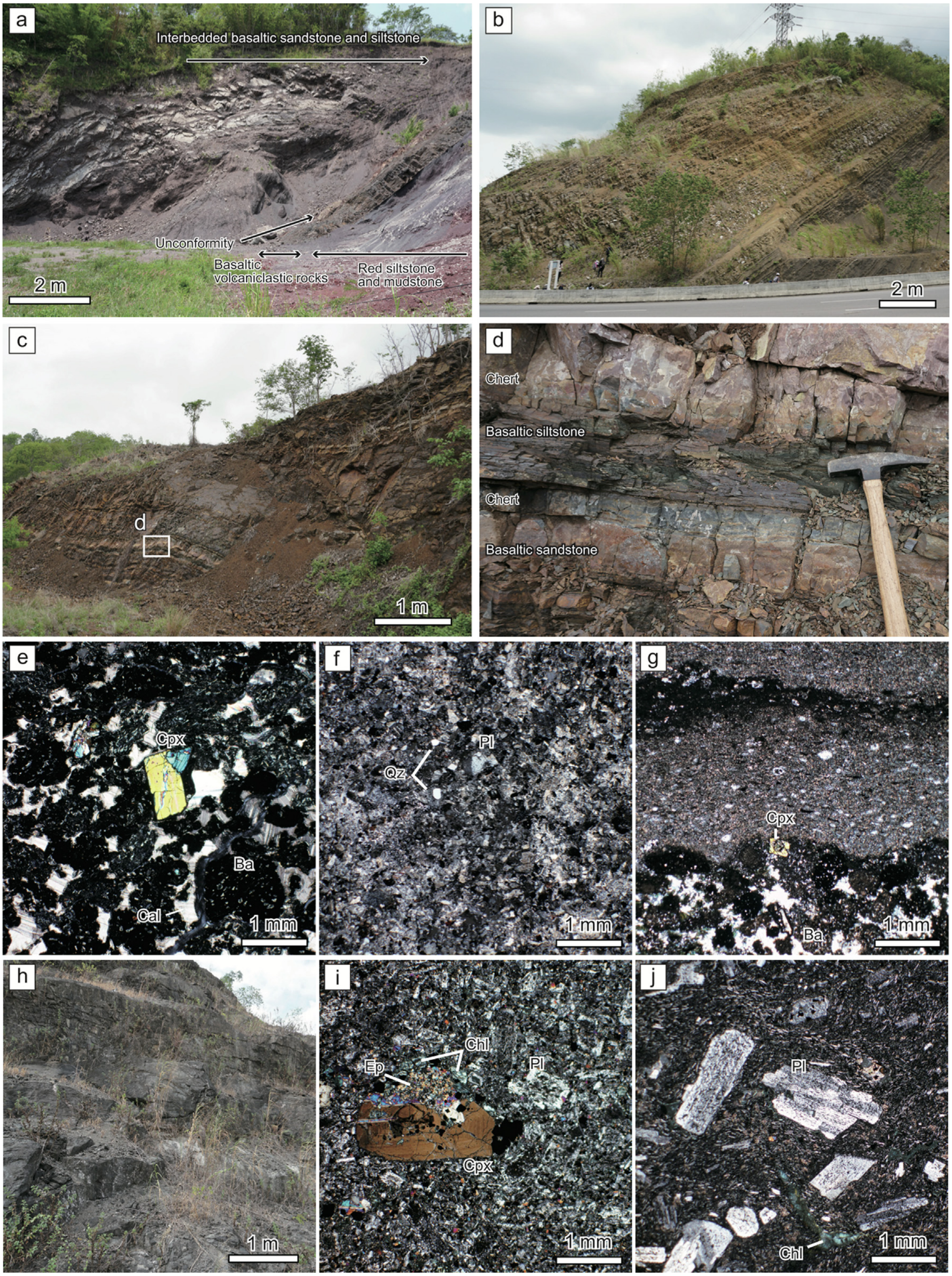

Fig. 8. Examples of the occurrence of basaltic sandstone and basalt. (a) Photograph of interbedded sandstone and siltstone (Loc. B450). (b) Photograph of interbedded sandstone and siltstone (Loc. B451). (c, d) Photograph of interbedded sandstone and siltstone with chert (Loc. B455). (e) Photomicrograph of basaltic sandstone composed of basaltic fragment and clinopyroxene with secondary calcite (Loc. B451). (f) Photomicrograph of basaltic sandstone composed of abundant plagioclase and minor quartz (Loc. B450). (g) Photomicrograph of interbedded sandstone and siltstone (Loc. B455). (h) Photograph of basalt (Loc. B487). (i) Photomicrograph of basalt with clinopyroxene and plagioclase phenocrysts (Loc. B487). (j) Photomicrograph of basalt with plagioclase phenocrysts (Loc. B495). Ba = basaltic fragment; Cal = calcite; Chl = chlorite; Cpx = clinopyroxene; Ep = epidote; Pl = plagioclase; Qz = quartz. Photomicrographs (e)–(g) and (i)–(j) taken under cross-polarized light.

youngest ages are presented in Table 1. The youngest mixture model ages are similar to the unmix ages. Isotopic data for the detrital zircon U–Pb dating are presented in Supplementary Data 3. Cathodoluminescence images and Concordia diagrams of detrital zircons are presented in Supplementary Data 4. Fig. 11 shows relative probability plots of all ages for the Huai Hin Lat, Nam Phong,

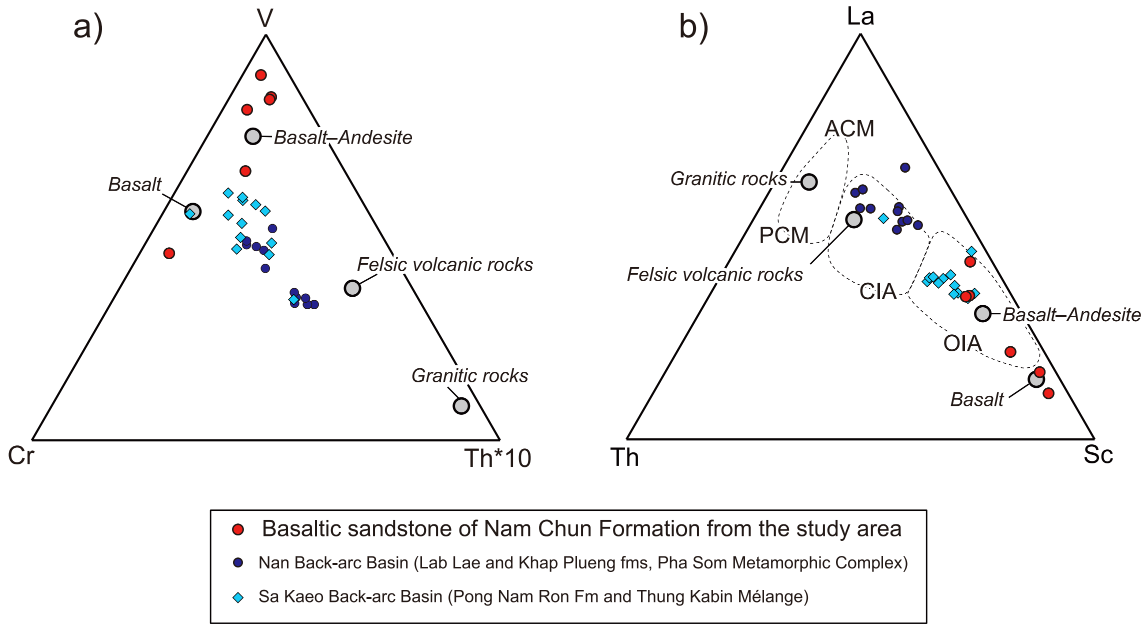

Fig. 9. Whole-rock geochemistry of basaltic sandstone. (a) V–Cr–Th*10 ternary diagram (Hara et al., 2018). (b) La–Th–Sc ternary diagram (Bhatia and Crook, 1986). OIA = oceanic island arc; CIA = continental island arc; ACM = active continental margin; PCM = passive continental margin. Data for basin-fill sediments of the Nan and Sa Kaeo Back-arc basins are from Hara et al. (2018, 2021). Average values for basalt–andesite and felsic volcanic rocks are from Srichan et al. (2009). The average value for basalt is from Hara et al. (2018). The average value for granitic rocks is after Phanerozoic granite from Condie (1993).

and Phu Kradung formations and associated conglomerates compiled from this study and Hara et al. (2021). Almost of all of the detrital zircons are characterized by multiple age clusters comprising Triassic and Paleozoic, and minor Proterozoic and Archean peaks (Fig. 11). These detrital zircons in Triassic sedimentary rocks of the Indochina Block were sourced from the collision zone between the Indochina and South China blocks, the Phetchabun Volcanic Belt (Hara et al., 2021). Most of the zircons are younger than 500 Ma (Fig. 11). Histograms and relative probability plots for zircons with ages younger than 500 Ma are presented in Fig. 12.

5.1. Type-1 conglomerates

Sandstone samples (449, T1, and T19) were collected from sandstone interbedded with Type-1 conglomerate and from sandstone matrix of Type-1 conglomerate at the Phu Nam Yod site. The detrital zircons are not abundant within these samples. Most of the detrital zircons separated from the samples can be grouped into multiple age clusters; i.e., Permian to Triassic (300–217 Ma), Devonian (400–350 Ma), and late Cambrian to Early Ordovician (500–450 Ma), with minor Proterozoic and Archean peaks (Fig. 11). The YC age is 250–217 Ma for the Huai Hin Lat Formation (Hara et al., 2021) and 310–280 Ma for Type-1 conglomerate. The youngest ages are 217 Ma (YSG) and 236 Ma (YC) for the Huai Hin Lat Formation, and 242–229 Ma (YSG), 243 Ma (YC of sample T19), and 261 and 251 Ma (unmix ages of samples T1 and 449, respectively) for Type-1 conglomerates (Fig. 12 and Table 1). The YSG ages for the Huai Hin Lat Formation and Type-1 conglomerates are consistent with the Late Triassic depositional age inferred from fossil data. In addition, the youngest ages of Type-1 conglomerates are slightly older than those of the Huai Hin Lat Formation because these conglomerates occupy the basal part of the formation.

5.2. Type-2 conglomerates

U–Pb ages of Type-2 conglomerates were obtained from three samples (377, 492, and FW1; Table 1). The dated samples were collected from sandstone interbedded with Type-2 conglomerate or from sandstone matrix in Type-2 conglomerate. The detrital zircons are not abundant within these samples. Detrital zircon ages from Type-2 conglomerates are characterized by Triassic (250–211 Ma), Carboniferous (350–300 Ma), and late Cambrian to Ordovician (500–450 Ma) clusters, with minor Proterozoic and Archean peaks (Fig. 11). The three samples of Type-2 conglomerate show youngest ages of 211–202 Ma (YSG), 237–228 Ma (YC), and 217–216 Ma (unmix age) (Fig. 12). The youngest ages for the Nam Phong Formation are 197 Ma (YSG) and 220 Ma (YC). The YSG age for the Nam Phong Formation is Early Jurassic, which is slightly younger than that indicated by fossil records (Hara et al., 2021). However, only one zircon grain indicates the Early Jurassic, the second YSG is 211 Ma presenting the latest Triassic. The depositional age of the Nam Phong Formation is assigned as the Rhaetian (latest Triassic), as determined by fossil evidence (Chonglakmani, 2011). In addition, the YSG and unmix ages of the Type-2 conglomerate are close to the Rhaetian (latest Triassic) depositional age of the Nam Phong Formation.

5.3. Phu Kradung Formation and Type-3 conglomerates

Detrital zircons from the Phu Kradung Formation (sample 378) and Type-3 conglomerate (sample 491) were dated (Table 1). The dated sample of Type-3 conglomerate was collected from sandstone interbedded with conglomerate. Almost all of the detrital zircons from both samples show U–Pb ages younger than 500 Ma, with a clear younger age population of the latest Triassic to Early Jurassic (Figs. 11 and 12). In addition, sample 378 from the Phu Kradung Formation shows a clear younger cluster of 270–240 Ma (middle Permian to Early Triassic; Fig. 12). The youngest ages of sample 378 are 180 Ma (YSG) and 201 Ma (YC) and those of sample 491 are 182 Ma (YSG) and 194 Ma (YC), indicating essentially identical ages for the Phu Kradung Formation and Type-3 conglomerates. These ages are Early Jurassic and substantially older than the Late Jurassic depositional age of the Phu Kradung Formation, as determined by fossil data excluding palynological data

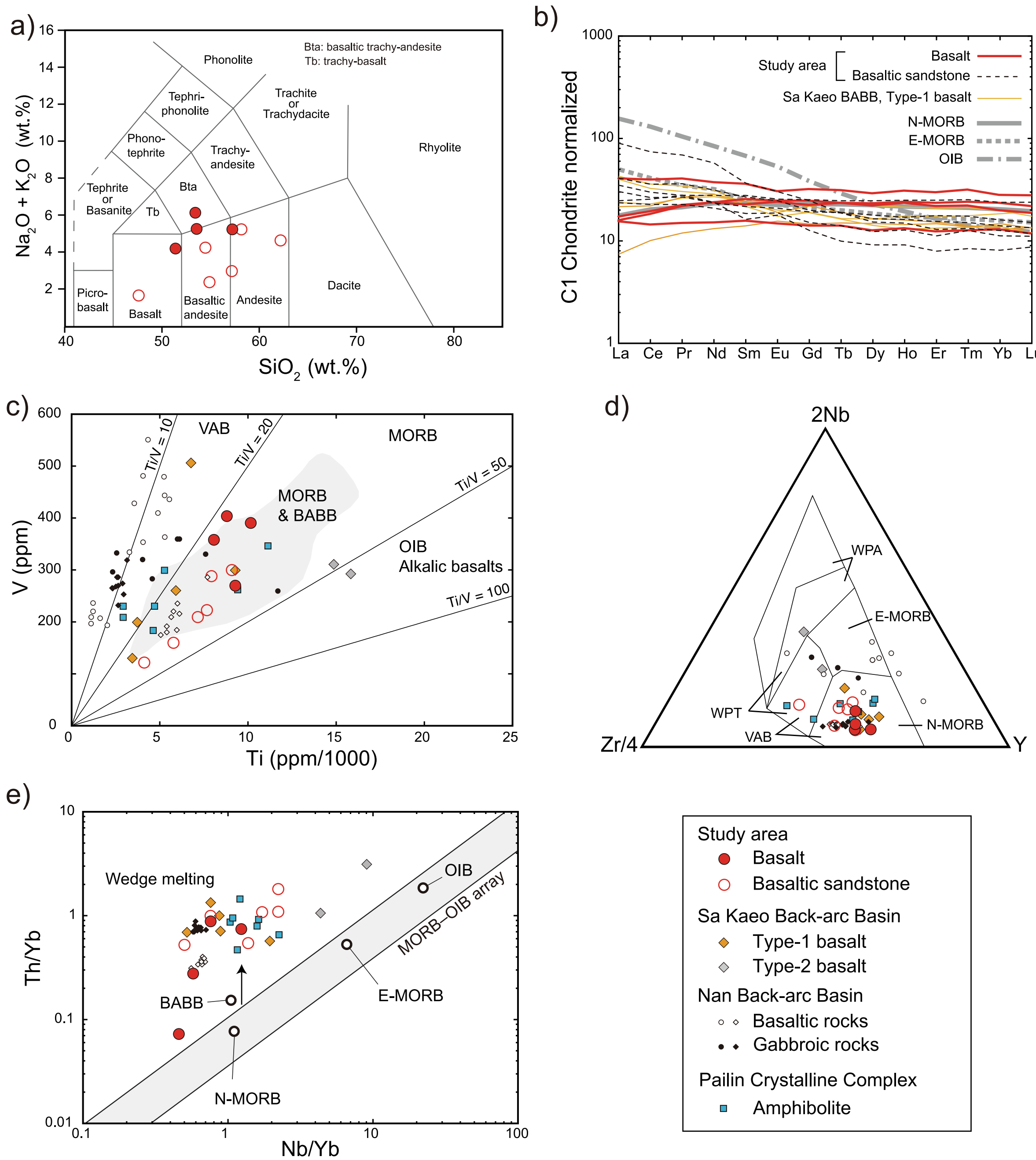

Fig. 10. Whole-rock geochemistry of basalt and basaltic sandstone. (a) SiO_2 versus $Na_2O + K_2O$ diagram (after Le Bas and Streckeisen, 1991). (b) C1-chondrite-normalized rare earth element contents. (c) Ti versus V diagram (after Shervais, 1982). (d) 2Nb–Zr/4–Y ternary diagram (after Meschede, 1986). (e) Nb/Yb versus Th/Yb diagram (after Pearce, 2008). N- and E-MORB = N- and E-type mid-ocean ridge basalt, respectively; OIB = ocean island basalt; VAB = volcanic arc basalt; BABB = back-arc basin basalt; WPA = within-plate basalt; WPT = within-plate tholeiite. C1 chondrite values are from McDonough and Sun (1995). N-MORB and E-MORB values are from Gale et al. (2013); OIB values are from Sun and McDonough (1989); Sa Kaeo Back-arc Basin basalt values are from Hara et al. (2018); Pailin Crystalline Complex values are from Hara et al. (2020); and Nan Back-arc Basin basalt values are from Macdonald and Barr (1984) and Barr and Macdonald (1987; black and white circles) and from Wang et al. (2020; black and white rhombi).

(Meesok and Saengsrichan, 2011). In this study, the depositional ages of the Phu Kradung Formation and Type-3 conglomerates are estimated to be younger than 201–180 Ma, based on the YSG and YC ages.

5.4. Basaltic sandstone

Detrital zircons of basaltic sandstone were collected from the Nam Chun Formation (sample 451). The detrital zircons are not abundant within these samples, usually presenting small grain size less than 100 μm. U–Pb ages of basaltic sandstone are characterized by a clear youngest age cluster of 240–200 Ma with minor Ordovician ages (Fig. 12). The basaltic sandstone sample has youngest ages of 206 Ma (YSG) and 216 Ma (YC) (latest Triassic; Table 1). These ages are interpreted as the maximum depositional age of the Nam Chun Formation, which lacks fossil evidence for its depositional age. The ages estimated for the basaltic sandstone are similar to those of Type-2 conglomerates. Basaltic sandstones of the Nam Chun Formation are assumed to have the same depositional age as that of Type-2 conglomerates (latest Triassic).

Table 1
Summary of samples and detrital zircon U–Pb ages.

Sample	Conglomerate/Formation	Latitude	Longitude	N	YSG age Ma ± 1σ	n	YC age Ma ± 1σ	Unmix age Ma ± 1σ	Mixture model age Ma ± 1σ
449	Type-1 conglomerate	1530′58.75″	10055′56.09″	77	236 ± 5	51	272 ± 3	251 ± 2	252 ± 1
T1	Type-1 conglomerate	1530′36.12″	10056′52.04″	39	229 ± 6	33	275 ± 5	261 ± 3	262 ± 2
T19	Type-1 conglomerate	1529′50.52″	10057′01.91″	39	242 ± 4	2	243 ± 6		
377	Type-2 conglomerate	1525′10.85″	10120′20.13″	74	206 ± 5	14	228 ± 4	217 ± 2	228 ± 1
492	Type-2 conglomerate	1513′05.93″	10118′47.91″	70	202 ± 5	47	234 ± 3	216 ± 2	216 ± 1
FW1	Type-2 conglomerate	1511′38.76″	10121′03.06″	33	211 ± 7	19	237 ± 9	216 ± 6	215 ± 3
B451	Nam Chun Formation	1646′43.29″	10107′02.18″	25	206 ± 6	13	216 ± 2		
378	Phu Kradung Formation	1523′36.88″	10121′31.90″	73	180 ± 7	12	201 ± 2		
491	Type-3 conglomerate	1516′27.82″	10121′41.16″	57	182 ± 7	40	194 ± 2		
485	Khok Kruat Formation	1649′35.68″	10055′44.84″	72	131 ± 5	2	134 ± 2		

The "unmix age" and the "mixture model" age were calculated using Isoplot v.4.15 (Ludwig, 2012) and DensityPlotter (Vermeesch, 2012).
YSG = youngest single grain; YC = youngest cluster; N = number of concordant data; n = number of grains used for YC age calculation.

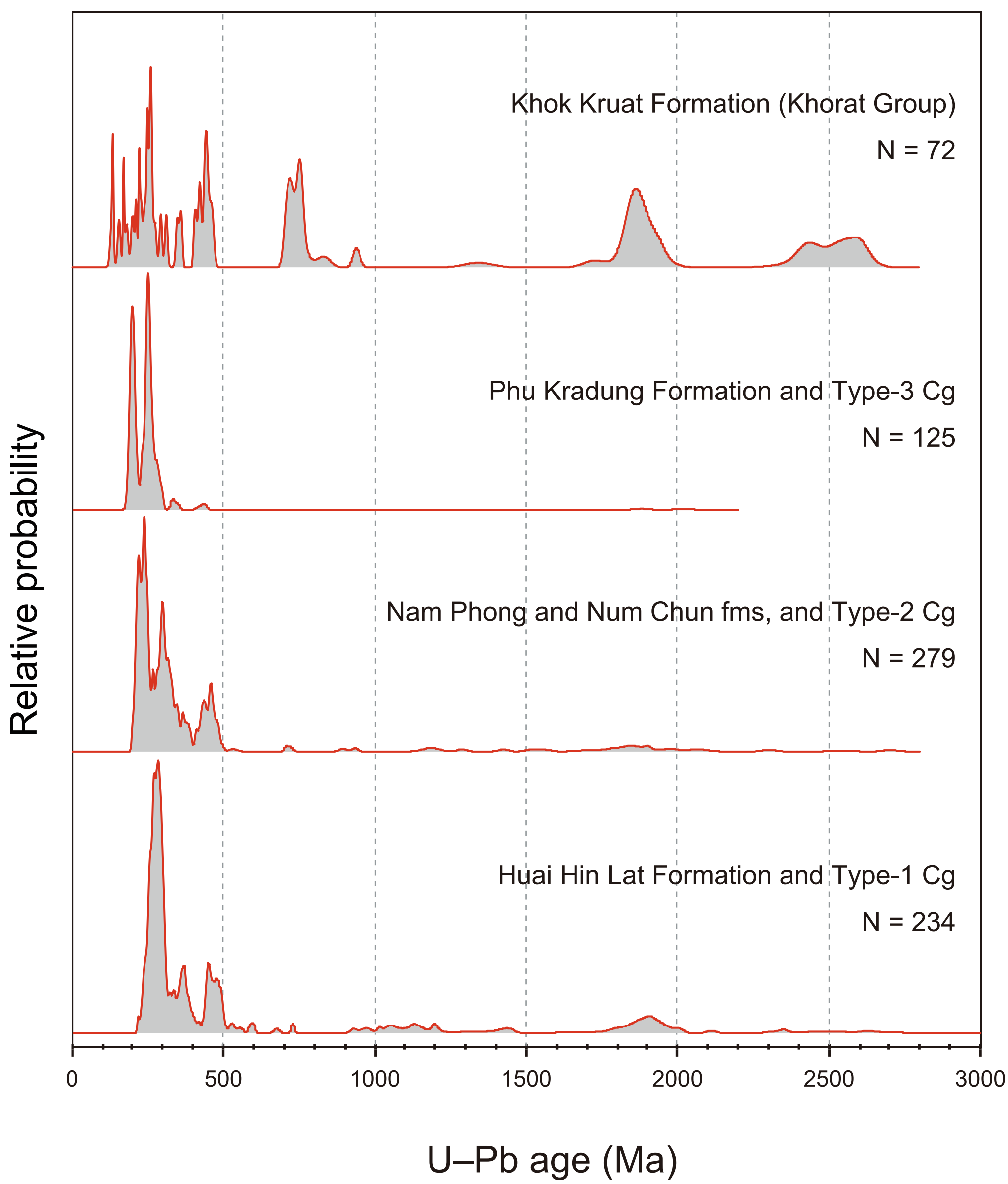

Fig. 11. Relative U–Pb age probability plots for the Khok Kruat Formation and for the Huai Hin Lat, Nam Phong, Nam Chun, and Phu Kradung formations and their equivalent conglomerates. Data are compiled from this study and Hara et al. (2021). Cg = conglomerate.

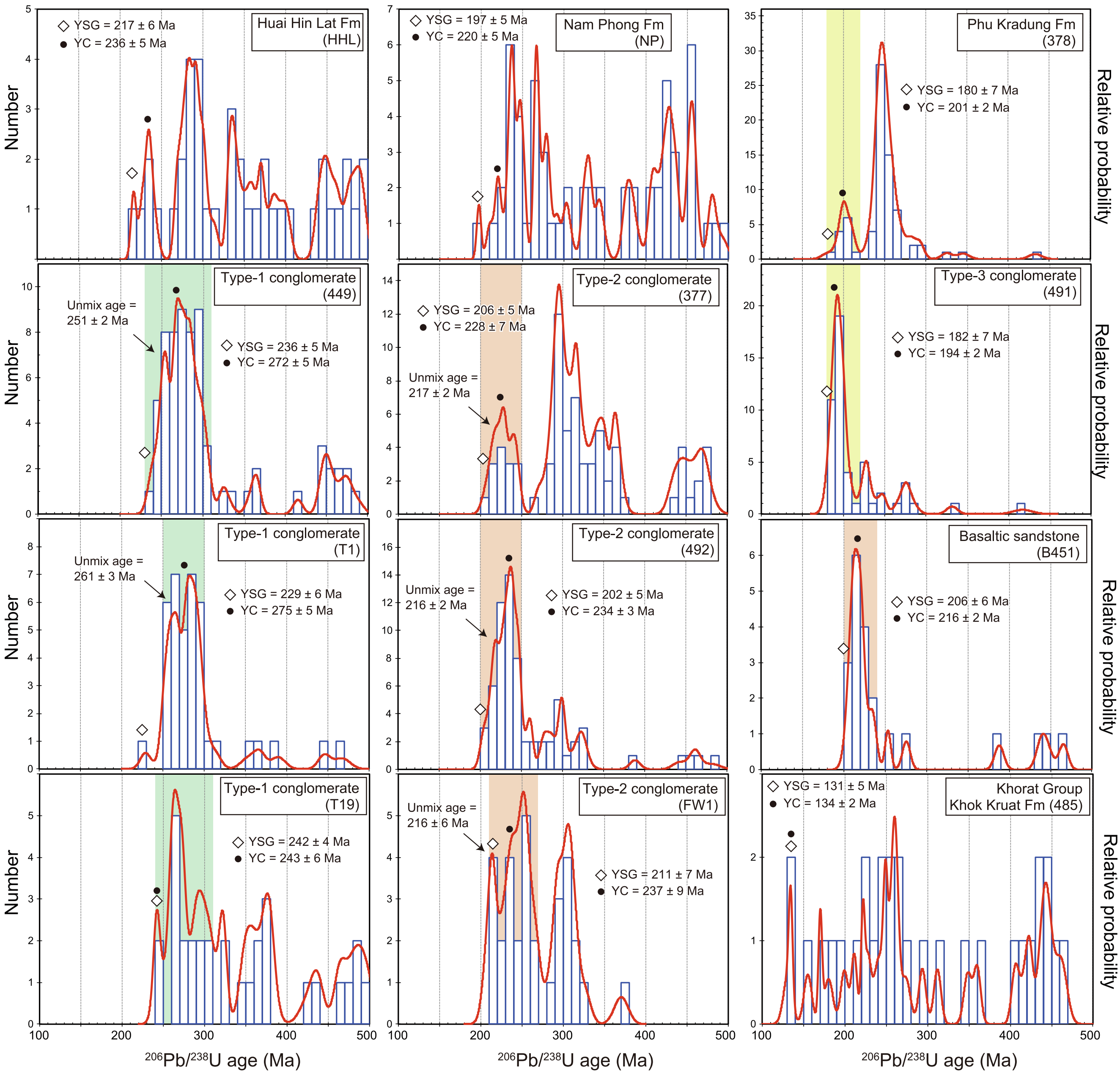

Fig. 12. $^{206}Pb/^{238}U$ age probability plots and distribution histograms for detrital zircons with ages of < 500 Ma. YSG = youngest single grain, YC = youngest cluster. Light-green, light-orange, and yellow shading denote the ranges of the younger age populations of Type-1 conglomerate, Type-2 conglomerate and basaltic sandstone, and Type-3 conglomerate and the Phu Kradung Formation, respectively.

5.5. Khok Kruat Formation of the Khorat Group

Sandstone for detrital zircon U–Pb dating was collected from the Early Cretaceous Khok Kruat Formation of the Khorat Group along Route 12 (sample 485). The Khok Kruat Formation is generally composed of quartzose sandstone, siltstone, mudstone, and conglomerate. Thick sandstone beds show predominant cross-bedding structure. The depositional age of this formation has been assigned as Aptian to Albian on the basis of fossil evidence (Meesok, 2011). The sandstone is characterized by detrital zircon ages ranging from 500 to 130 Ma, with Proterozoic and Archean peaks (Fig. 11). The youngest detrital zircon U–Pb ages are 131 Ma (YSG) and 134 Ma (YC)—i.e., Valanginian to Hauterivian (Fig. 12 and Table 1)—and are slightly older than the depositional age of Aptian to Albian.

6. Reconstruction of the Indosinian Orogeny

The Indosinian Orogeny has been identified as comprising three events during the Early to Middle Triassic (Event I), Late Triassic (Event II), and Early to Middle Jurassic (Event III), as evidenced by major unconformities within the Triassic to Jurassic sedimentary rocks in the subsurface geology of the Khorat Basin (Booth and Sattayarak, 2011). In this section, we reconstruct Indosinian I, II, and III events on the basis of the occurrence and characteristics of the studied conglomerates and their detrital U–Pb ages from our investigation of the surface geology in the Phetchabun–Lamnarai areas. In addition, we summarize the stratigraphy and youngest detrital zircon U–Pb ages (Fig. 13), and also discuss the Indosinian Orogeny with respect to sediment provenance and in the context of collision and subduction tectonics that occurred in Southeast Asia.

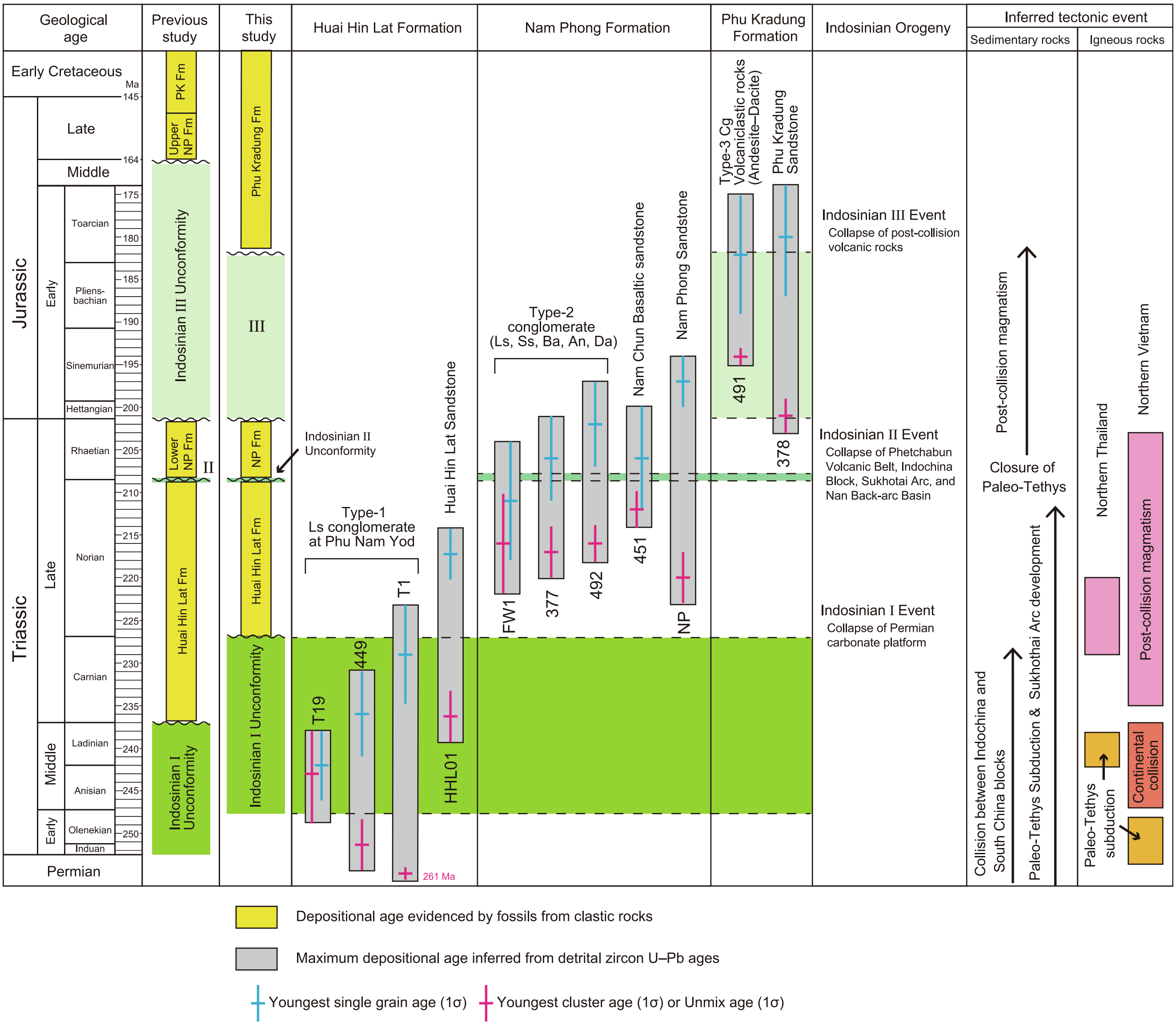

Fig. 13. Summary stratigraphic column showing depositional ages and detrital zircon U–Pb ages for the Indochina Block and related to the Indosinian Orogeny. Previous study is modified after Racey (2009) and Booth and Sattayarak (2011). Periods of igneous activities are based on Qian et al. (2016) and Wang et al. (2018) for Northern Thailand, Liu et al. (2018) for Northern Vietnam. An = andesite; Ba = basalt; Da = dacite; Fm = formation; Ls = limestone; Ss = sandstone; NP = Nam Phong; PK = Phu Kradung.

6.1. Indosinian I Event

In the subsurface study, the Indosinian I Unconformity is recognized between the Permian Saraburi Group and the Late Triassic Huai Hin Lat Formation (Kuchinarai Group in the subsurface geology) and represents a hiatus during the Early–Middle Triassic (Fig. 13; Booth and Sattayarak, 2011). This unconformity, which is identified as a major unconformity in the subsurface geology, is inferred to have formed by uplift and erosion associated with compressional deformation of the Carboniferous and Permian platform carbonates of the Saraburi Group (Booth and Sattayarak, 2011). These Carboniferous and Permian sediments are estimated to have undergone more than 2000 m of erosion of the rock column (Minezaki et al., 2019). The Indosinian I Event, as deduced from the vertical section corresponding to this unconformity, is considered to have been the main tectonic event of the Indosinian Orogeny. The Type-1 conglomerates were derived mostly from collapse of the Permian carbonate platform during the Indosinian I Event (Fig. 14). Minor clasts composed of igneous and sedimentary rocks within the Type-1 conglomerates were probably derived from basement rocks of the Indochina Block.

The main event, Indosinian I, is inferred to have occurred during the earliest Triassic to early Middle Triassic (Booth and Sattayarak, 2011) or the Middle to early Late Triassic (Morley et al., 2013; Minezaki et al., 2019) on the basis of the associated geological and tectonic events. In the present study, the Indosinian I Event is represented by Type-1 conglomerate, which is composed mostly of limestone with minor basalt, fine-grained porphyritic granite, and sedimentary rocks. The youngest detrital zircon ages of Type-1 conglomerates are 242–229 Ma (YSG) and 275–243 Ma (YC). Adopting the detrital zircon YSG age as the depositional age and fossil evidence, the Type-1 conglomerate is estimated to have formed during the middle Late Triassic (Norian), which corresponds to the period of the Indosinian I Event proposed by Morley et al. (2013) and Minezaki et al. (2019).

The KKFTB in the southwestern Indochina Block consists of a Permian carbonate platform with clastic rocks of the Saraburi Group and was deformed during the Middle to Late Triassic stage

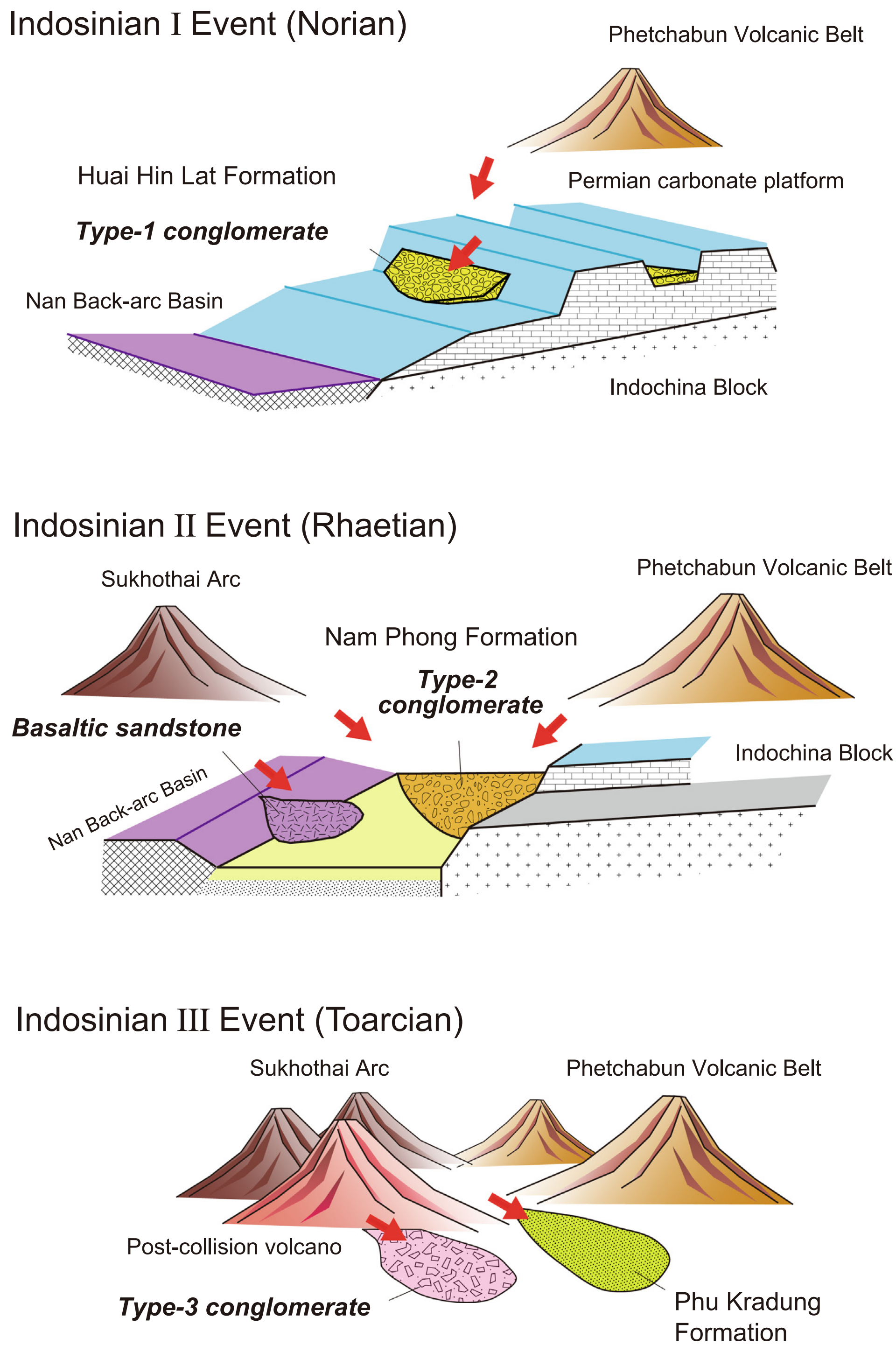

Fig. 14. Schematic model of the formation of Type-1, Type-2, and Type-3 conglomerates during the Indosinian Orogeny. See the text for details (Section 6). Red arrows present sediment supply direction.

of the Indosinian Orogeny (Morley et al., 2013). Results of structural analysis, zircon U–Pb ages, illite K–Ar ages, and calcite U–Pb ages have allowed two stages of deformation to be identified in the KKFTB, related to Indosinian I and II events, respectively (Morley et al., 2013, 2022; Arboit et al., 2014, 2015, 2016a, b; Hansberry et al., 2014, 2017; Simpson et al., 2021). The first deformation stage is represented by predominant WNW–ESE-striking thrust-and-fold structures resulting from collision between the South China and Indochina blocks These structures have also been interpreted in ribbon continents and in Zealandia (Morley et al., 2022). The second stage is represented by N–S-trending sutures formed by collision between the Indochina and Sibumasu blocks. In addition, the compression involved in the continental collision formed horst-and-half-graben systems in Carboniferous and Permian sedimentary rocks in the subsurface of the Khorat Basin, showing NW–SE trends in the northeastern part of the basin and E–W trends in the southern part (Minezaki et al., 2019). Thus, the Indosinian I Unconformity was characterized by compression tectonics during the Anisian to Carnian as a result of collision between the South China and Indochina blocks (Minezaki et al., 2019).

At the time of the Indosinian I Event, the Sukhothai Arc along the western Indochina Block underwent intensive igneous activity, the development of forearc basins, and the filling of back-arc basins with sediments (Hara et al., 2021). Paleo-Tethyan subduction is considered to be probably limited to tectonism involved in the development of the Sukhothai Arc during this period and did not affect the Indochina Block.

6.2. Indosinian II Event

The Indosinian Ⅱ Unconformity was identified between the Huai Hin Lat and Nam Phong formations (Fig. 13). The hiatus associated with the Indosinian Ⅱ Unconformity was a short period at the Norian and Rhaetian boundary (Booth and Sattayarak, 2011). The Indosinian II Event caused subsidence of half-graben basins by the development of an extensional field in the Khorat Basin and was weaker than the Indosinian I Event (Booth and Sattayarak, 2011; Minezaki et al., 2019). In this study, the Indosinian II Event is represented by Type-2 conglomerates in the surface geology. The Type-2 conglomerates are characterized by clasts of varied lithology, including limestone, sandstone, mudstone, basalt, andesite, and dacite, implying variation in provenance. Geochemical data suggested that almost of volcanic clasts were provided from both of the Phetchabun Volcanic Belt and the Sukhothai Arc (Fig. 4c). The depositional age of Type-2 conglomerates is inferred to be 211–202 Ma or younger, as indicated by the youngest detrital zircon age estimated from the YSG ages (Fig. 10). This estimated depositional age is Rhaetian, corresponding to the period of the Indosinian II Event.

A Middle Triassic (242–238 Ma) subduction-related igneous event and a Late Triassic (229–220 Ma) post-collision igneous event have been proposed on the basis of the geochemistry and zircon U–Pb ages of igneous rocks from the Sukhothai Arc (Qian et al., 2016; Wang et al., 2018). The Late Triassic post-collision igneous event is considered to have been caused by collision between the Sibumasu Block, the Sukhothai Arc, and the Indochina Block (Qian et al., 2016; Wang et al., 2018). However, turbidite- and carbonate-dominant facies of the Song Group continued to be deposited within the forearc basin of the Sukhothai Arc during the Late Triassic (Hara et al., 2017). The turbidite-dominant Wang Chin Formation of the Song Group has a depositional age of middle Carnian to early Norian based on bivalves, ammonoids, and conodonts (Chonglakmani, 2011), and the detrital zircon YSG age for the formation is Norian (Hara et al., 2017), although foraminifera of Norian to Rhaetian age have been reported from limestone (Miyahigashi, 2014). In addition, the deposition of basin-fill sediments within the Nan Back-arc Basin also continued into the middle Norian, as evidenced by detrital zircon YSG and YC ages (Hara et al., 2021). Thus, the post-collision igneous event proposed by Qian et al. (2016) must have started during deposition of the forearc and back-arc sediments. Here, we accept the geological record of sedimentary events associated with the development of the Sukhothai Arc, meaning that the closure of the Paleo-Tethys occurred around the Norian–Rhaetian boundary and that the post-collisional event commenced after the Rhaetian. In addition, the clasts with varied lithology and containing diverse and abundant Paleozoic zircons were derived from basement rocks of the Indochina Block and the Phetchabun Volcanic Belt, as well as the Sukhothai Arc, all of which were uplifted during the Indosinian II Event (Fig. 14). These sedimentological signatures suggest that the Indosinian II Event was triggered by the closure of the Paleo-Tethys and collision between the Sibumasu Block, the Sukhothai Arc, and the Indochina Block, consistent with N–S-trending structures in the Permian Saraburi Group (Morley et al., 2013, 2022; Minezaki et al., 2019).

The basaltic sandstones of the Nam Chun Formation were deposited contemporaneously with Type-2 conglomerates, as indicated by the youngest detrital zircon ages of 216–206 Ma estimated from the YSG and YC ages for this formation (Fig. 12 and Table 1). The studied basaltic sandstones and basalts have similar geochemical characteristics to those of Type-1 basalt of the Sa Kaeo Back-arc Basin and amphibolite of the Pailin Crystalline Complex (Fig. 10). The present study area is located in the western Indochina Block, behind the Nan Back-arc Basin. Our field observations and geochemical results suggest that the basaltic sandstones were derived directly from the Nan Back-arc Basin and that the associated basalts exposed near the basaltic sandstones may have corresponded in nature with the Nan Back-arc Basin basalts. Thus, the Nam Chun basaltic sandstones are interpreted as collapse sediments of the Nan Back-arc Basin that formed during the Indosinian II Event (Fig. 14). In summary, the Indosinian II Event involved uplift of the Sukhothai Arc, the Phetchabun Volcanic Belt, the Indochina Block, and the Nan Back-arc Basin, followed by their collapse and then commencement of collision between the Sibumasu and Indochina blocks after closure of the Paleo-Tethys during the latest Triassic (Norian–Rhaetian boundary).

6.3. Indosinian III Event

The Indosinian III Event is defined by the Indosinian Ⅲ Unconformity between the Lower and Upper Nam Phong Formation in the subsurface of the Khorat Basin (Fig. 13). Lithologies of the Lower and Upper Nam Phong Formation present similar associations of interbedded shales, siltstones, and sandstones, bounded by a subhorizontal unconformity. The Indosinian III Event has been identified on only a few seismic profiles in the Khorat Basin and has not been associated with a major tectonic event (Booth and Sattayarak, 2011; Minezaki et al., 2019). In addition, the Nam Phong Formation has not been divided into Lower and Upper in the surface geology. Although geological evidences are weak for the Indosinian III Event, the intervening unconformity indicates a prolonged hiatus of 45–50 Myr during the Early to Middle Jurassic (Racey and Goodall, 2009; Booth and Sattayarak, 2011). Despite the Indosinian III Event being poorly understood, we focus here on Type-3 conglomerates and the Phu Kradung Formation in the Lamnarai area, which are interpreted as sediments produced during the Indosinian III Event.

The Type-3 conglomerates are characterized by volcaniclastic rocks and volcanic breccias composed of andesite and dacite from granules, pebbles, to cobbles in size. Based on geochemical data, almost of volcanic clasts were sourced from post-collision volcanic rocks (Fig. 4c). The YSG age of detrital zircons constrain the maximum depositional age of this conglomerate to 182 Ma or younger (Early Jurassic). In addition, sandstones of the Phu Kradung Formation, which contain abundant lithic fragments of volcanic rocks, have a similar maximum depositional age of 180 Ma. These ages are substantially older than the Late Jurassic–Early Cretaceous depositional age estimated from fossils of the Phu Kradung Formation. These older ages suggest that *syn*-depositional zircons are absent from the Phu Kradung Formation. However, the Early Cretaceous Khok Kruat Formation, which is stratigraphically the upper part of the Phu Kradung Formation in the Khorat Group (Fig. 3), contains Early Cretaceous zircons with a YSG age of 131 Ma and a YC age of 134 Ma, as well as Jurassic zircons (Fig. 12). The presence of Jurassic to Early Cretaceous zircons in the Khorat Group suggests that *syn*-depositional zircons may have been transported into the Phu Kradung Formation at the time of sedimentation. Assuming that the YSG ages are within the range of the depositional age, the Phu Kradung Formation may have been deposited during the late Early Jurassic. Accordingly, we propose that the Indosinian III Unconformity occurred during the Early Jurassic (201–182 Ma) after the deposition of the Nam Phong Formation but before that of the Phu Kradung Formation, as estimated by the youngest detrital zircon age. The duration of the hiatus corresponding to the Indosinian Ⅲ Unconformity is calculated at 20 Myr, based on detrital zircon U–Pb age clarified in this study.

In addition, in this study, the maximum depositional age of the Phu Kradung Formation in the Lamnarai area has been revised to the late Early Jurassic (Toarcian), inferred from the youngest zircon YSG ages. The Early Jurassic Phu Kradung Formation in this area probably corresponds to part of the Upper Nam Phong Formation of the Khorat Basin in the subsurface, as the older limit of the depositional age of the Upper Nam Phong Formation is the Pliensbachian, as determined by palynological data (Racey and Goodall, 2009), suggesting a similar depositional age to that inferred from our detrital zircon ages. Alternatively, the Early Jurassic Phu Kradung Formation in the Lamnarai area could be assigned a new formation name after further study.

A post-collision volcanic event took place between the Sibumasu and Indochina blocks during the Late Triassic (229–220 Ma) in northern Thailand (Qian et al., 2016). As mentioned above, the main post-collision event occurred later, as judged from sedimentary evidence within the Sukhothai Arc. In addition, S-type granitoids in the Main Range Province (or Central Belt) were emplaced during the early Late Triassic to Early Jurassic (Cobbing et al., 1986; Charusiri et al., 1993; Cobbing, 2011) and were generated as a result of collision between the Sibumasu Block, the Sukhothai Arc, and the Indochina Block during 230–180 Ma (Sone and Metcalfe, 2008), 219–198 Ma (Searle et al., 2012), or 227–200 Ma (Gardiner et al., 2016). Metamorphic rocks from the Sibumasu Block and the Sukhothai Arc have yielded zircon U–Pb ages of 230–185 Ma during the early Late Triassic to Early Jurassic (Dunning et al., 1995; Kawakami et al., 2014). Recently, new radiometric data for the Late Triassic to Early Jurassic have been reported for igneous rocks from the Phetchabun Volcanic Belt (Nualkhao et al., 2018) and volcanic rocks from the Sukhothai Arc (Srichan, 2019). K–Ar ages of igneous rocks were estimated to be 221–171 Ma by Nualkhao et al. (2018). U–Pb ages of volcanic rocks reported by Srichan (2019) range from 230 to 184 Ma and are consistent with the youngest detrital zircon YSG and YC ages (201–180 Ma) of Type-3 conglomerate and sandstone of the Phu Kradung Formation. Thus, we consider that the post-collision magmatism occurred during the Hettangian to Toarcian (Early Jurassic). In addition, Type-3 conglomerates were deposited after the Toarcian (late Early Jurassic), that sourced directly from the Early Jurassic post-collision volcanic rocks (Fig. 14).

6.4. Unresolved problem for the timing of the Paleo-Tethys closure

As mentioned above, we discussed that the Paleo-Tethys subduction continued until the latest Triassic and that the post-collisional event occurred during the Early Jurassic, based on sedimentary records within the Indochina Block and the Sukhothai Arc. Our tectonic conclusions are coincident with previous models provided from sedimentary rocks in subsurface and surface geology in the Indochina Block(e.g., Booth and Sattayarak, 2011; Minezaki et al., 2019; Morley et al., 2013, 2022). On the other hand, two stages of igneous events have been accepted: 1) Middle Triassic (242–238 Ma) subduction-related igneous event; 2) Late Triassic (229–220 Ma) post-collision igneous event, based on the geochemistry and zircon U–Pb ages of igneous rocks from the Sukhothai Arc (e.g., Qian et al., 2016; Wang et al., 2018). Assuming that the Indosinian Orogeny was provided by these igneous events, the Indosinian I and II events were caused by the Paleo-Tethys closure and the post-collision magmatism, and the Indosinian III Event might be related to the latest post-collision magmatism. However, this tectonic history does not correspond to the sedimentary records of the Triassic to Early Jurassic Khorat Basin in the western Indochina Block, the Permian to Late Triassic forearc and back-arc basins in the Sukhothai Arc (Booth and Sattayarak, 2011; Minezaki et al., 2019; Hara et al., 2021). In addition, the Early to Late Triassic marine and hemipelagic sediments of the Mae Sariang Group were deposited along the eastern margin of the Sibumasu Block (Kamata et al., 2022; Srinak et al., 2007; Hara et al., 2021), suggesting that the Paleo-Tethys was still opened between the Sibumasu Block and the Sukhothai Arc during the Triassic. Thus, timing of the Paleo-Tethys closure has unresolved problem between sedimentary and igneous rocks. This problem is due to the lack of studies linking geological phenomena between sedimentary record and igneous activity. The igneous clasts within the conglomerates might provide a clue to resolve this problem, although further studies are needed.

7. Conclusion

We investigated the Indosinian Orogeny as recorded in the western Indochina Block by conglomerates and detrital zircon U–Pb ages from the Phetchabun–Lamnarai area, central Thailand. We identified Events I, II, and III of the Indosinian Orogeny on the basis of the surface geology. These events were associated with Paleo-Tethyan subduction and micro-continental collision tectonics. Our main conclusions are as follows:

1. The Indosinian I Event is represented by Type-1 limestone conglomerates, whose formation was a result of collapse of the Permian carbonate platform. This event occurred during the Late Triassic (Norian) and was triggered by collision between the Indochina and South China blocks.
2. The Indosinian II Event is represented by Type-2 conglomerates, which are composed of various clasts and basaltic sandstones derived from the collapse of the Sukhothai Arc, the Nan Back-arc Basin, the Phetchabun Volcanic Belt, and basement rocks of the Indochina Block. This event was caused by the closure of the Paleo-Tethys and the commencement of collision between the Sibumasu Block, the Sukhothai Arc, and the Indochina Block at the latest Triassic (Rhaetian).
3. The Indosinian III Event is represented by Type-3 conglomerates, which comprise volcaniclastic rocks and volcanic breccias composed of andesite and dacite. This event occurred the late Early Jurassic (Toarcian or younger) was associated with post-collision magmatism that occurred between the Sibumasu and Indochina blocks.

CRediT authorship contribution statement

Hidetoshi Hara: Conceptualization, Investigation, Writing – original draft. **Thasinee Charoentitirat:** Conceptualization, Investigation, Writing – review & editing. **Tetsuya Tokiwa:** Investigation, Data curation, Writing – review & editing. **Toshiyuki Kurihara:** Investigation, Writing – review & editing. **Keisuke Suzuki:** Investigation, Data curation. **Apsorn Sardsud:** Investigation, Writing – review & editing.

Declaration of competing interest

The authors declare that they have no known competing financial interests or personal relationships that could have appeared to influence the work reported in this paper.

Acknowledgments

We thank Prof. P. Charusiri, Prof. K. Hisada, Prof. K. Ueno, Dr. Y. Kamata, and Dr. T. Minezaki for valuable comments on the geology and tectonics of Thailand, Prof. K. Yamamoto and Dr. K. Shimura for support during zircon U–Pb dating at Nagoya University, and Ms. R. Nohara for assistance during geochemical analysis at Niigata University. We are grateful to Ms. C. Phuchareanchaiwon, Ms. C. Pothichiya, Mr. R. Leotphayakkarat, Ms. I. Chanpheng, Ms. T. Pengtha, and Ms. P. Khamfoo for their support during field surveys and sampling, and to staff of the thin-section preparation laboratory at the Geological Survey of Japan for their assistance. This research is partly funded by Fossil Management Fund Division's research project in 2020, Department of Mineral Resources, Thailand. Thanks are also due to Prof. Y. Dong and anonymous reviewers for constructive and valuable comments on the manuscript.

Appendix A. Supplementary data

Supplementary data to this article can be found online at https://doi.org/10.1016/j.gr.2023.11.009.

References

Aitchison, J.C., Davis, A.M., Badengzhu, Luo, H., 2002. New constraints on the India–Asia collision: the Lower Miocene Gangrinboche conglomerates, Yarlung Tsangpo suture zone. SE Tibet. J. Asian Earth Sci. 21, 251–263.
Arboit, F., Collins, A.S., King, R., Morley, C.K., Hansberry, R., 2014. Structure of the Sibumasu-Indochina collision, central Thailand: a section through the Khao Khwang Fold and thrust belt. J. Asian Earth Sci. 95, 182–191.
Arboit, F., Amrouch, K., Collins, A.S., King, R., Morley, C., 2015. Determination of the tectonic evolution from fractures, faults and calcite twins on the southwestern margin of the Indochina Block. Tectonics 34, 1576–1599.
Arboit, F., Collins, A.S., Morley, C.K., King, R., Amrouch, K., 2016a. Detrital zircon analysis of the southwest Indochina terrane, central Thailand: unravelling the Indosinian orogeny. Geol. Soc. Amer. Bull. 128, 1024–1043.
Arboit, F., Collins, A.S., Morley, C.K., Jourdan, F., King, R., Foden, J., Amrouch, K., 2016b. Geochronological and geochemical studies of mafic and intermediate dykes from the Khao Khwang Fold-Thrust Belt: implications for petrogenesis and tectonic evolution. Gondwana Res. 36, 124–141.
Barber, A.J., Ridd, M.F., Crow, M.J., 2011. The origin, movement and assembly of the pre-Tertiary tectonic units of Thailand. In: Ridd, M.F., Barber, A.J., Crow, M.J. (Eds.), The Geology of Thailand. Geol. Soc, London, pp. 507–537.
Barr, S.M., Charusiri, P., 2011. Volcanic rocks. In: Ridd, M.F., Barber, A.J., Crow, M.J. (Eds.), The Geology of Thailand. Geol. Soc, London, pp. 415–439.
Barr, S.M., Macdonald, A.S., 1987. Nan River suture zone, northern Thailand. Geology 15, 907–910.
Barr, S.M., Macdonald, A.S., Dunning, G.R., Ounchanum, P., Yaowanoiyothin, W., 2000. Petrochemistry, U-Pb (zircon) age, and palaeotectonic setting of the Lampang volcanic belt, northern Thailand. J. Geol. Soc. London 157, 553–563.
Barr, S.M., Macdonald, A.S., Ounchanum, P., Hamilton, M.A., 2006. Age, tectonic setting and regional implications of the Chiang Khong volcanic suite, northern Thailand. J. Geol. Soc London 163, 1037–1046.
Barrett, T.J., MacLean, W.H., 1999. Volcanic sequences, lithogeochemistry, and hydrothermal alteration in some bimodal volcanic-associated massive sulfide systems. In: Barrie, C.T., Hannington, M.D. (Eds.), Volcanic-associated Massive Sulfide Systems: Processes and Examples in Modern and Ancient Settings. Rev. Econ. Geol., 8, 101–131.
Bhatia, M.R., Crook, K.A.W., 1986. Trace element characteristics of graywackes and tectonic setting discrimination of sedimentary basins. Contrib. Miner. Petrol. 92, 181–193.
Boonsoong, A., Panjasawatwong, Y., Metparsopsan, K., 2011. Petrochemistry and tectonic setting of mafic volcanic rocks in the Chon Daen-Wang Pong area, Phetchabun, Thailand. Island Arc 20, 107–124.
Booth, J., Sattayarak, N., 2011. Subsurface Carboniferous-Cretaceous geology of NE Thailand. In: Ridd, M.F., Barber, A.J., Crow, M.J. (Eds.), The Geology of Thailand. Geol. Soc, London, pp. 185–222.
Burrett, C., Udchachon, M., Thassanapak, H., 2021. The Truong Son, Loei-Phetchabun, and Kontum Terranes in Indochina: provenance, rifting, and collisions. Front. Earth Sci. 9, 603565.
Campbell, M.J., Hoy, D., Rosenbaum, G., Fielding, C., Allen, C.M., 2022. The onset of Gondwanide Orogeny in Eastern Australia: insight from the provenance of syn-orogenic strata in the New England Orogen (Australia). Tectonics 41.
Carter, A., Clift, P.D., 2008. Was the Indosinian orogeny a Triassic mountain building or a thermotectonic reactivation event? C. R. Geosci. 340, 83–93.
Carter, A., Roques, D., Bristow, C., Kinny, P., 2001. Understanding Mesozoic accretion in Southeast Asia: significance of Triassic thermotectonism (Indosinian orogeny) in Vietnam. Geology 29, 211–214.
Chairangsee, C., Assavapatchara, S., 2009. Geological Map of Changwat Loei (Scale 1:250,000). Department of Mineral Resources, Bangkok.
Charusiri, P., Clark, A.H., Farrar, E., Archibald, D., Charusiri, B., 1993. Granite belts in Thailand: evidence from the $^{40}Ar/^{39}Ar$ geochronological and geological syntheses. J. SE Asian Earth Sci. 8, 127–136.
Chonglakmani, C., 2011. Triassic. In: Ridd, M.F., Barber, A.J., Crow, M.J. (Eds.), The Geology of Thailand. Geol. Soc, London, pp. 137–150.
Chonglakmani, C., Satayarak, N., 1984. Geological Map of Changwat Phetchabun (Sheet NE 47–16, Scale 1:250,000). Department of Mineral Resources, Bangkok.
Cobbing, E.J., 2011. Granitic rocks. In: Ridd, M.F., Barber, A.J., Crow, M.J. (Eds.), The Geology of Thailand. Geol. Soc, London, pp. 441–457.
Cobbing, E.J., Mallick, D.I.J., Pitfield, P.E.J., Teoh, L.H., 1986. The granites of the Southeast Asia Tin Belt. J. Geol. Soc. London 143, 537–550.
Condie, K.C., 1993. Chemical composition and evolution of the upper continental crust: contrasting results from surface samples and shales. Chem. Geol. 104, 1–37.
Cuny, G., Liard, R., Deesri, U., Liard, T., Khamha, S., Suttethorn, V., 2014. Shark faunas from the Late Jurassic-Early Cretaceous of northeastern Thailand. Paläontol. Z. 88, 309–328.
Department of Mineral Resources, 1999. Geological Map of Thailand. Scale 1:1,000,000, Geological Survey Division, Department of Mineral Resources, Bangkok.
Dunning, G.R., Macdonald, A.S., Barr, S.M., 1995. Zircon and monazite U-Pb dating of the Doi Inthanon core complex, northern Thailand: implications for extension within the Indosinian Orogen. Tectonophysics 251, 197–213.
Faure, M., Lepvrier, C., Nguyen, V.V., Vu, T.V., Lin, W., Chen, Z., 2014. The South China block-Indochina collision: Where, when, and how? J. Asian Earth Sci. 79, 260–274.
Gale, A., Dalton, C.A., Langmuir, C.H., Su, Y., Schilling, J., 2013. The mean composition of ocean ridge basalts. Geochem. Geophys. Geosys. 14, 489–518.
Gardiner, N.J., Searle, M.P., Morley, C.K., Whitehouse, M.P., Spencer, C.J., Robb, L.J., 2016. The closure of Palaeo-Tethys in Eastern Myanmar and Northern Thailand: new insights from zircon U-Pb and Hf isotope data. Gondwana Res. 39, 401–422.
Hansberry, R.L., King, R., Collins, A.S., Morley, C.K., 2014. Complex structure of an upper-level shale detachment zone: Khao Khwang fold and thrust belt, central Thailand. J. Struct. Geol. 67, 140–153.
Hansberry, R.L., Collins, A.S., King, R.C., Morley, C.K., Giże, A.P., Warren, J., Löhr, S.C., Hall, P.A., 2015. Syn-deformation temperature and fossil fluid pathways along an exhumed detachment zone, Khao Khwang fold-thrust belt, Thailand. Tectonophysics 655, 73–87.
Hansberry, R.L., Zwingmann, H., Loehr, S., Collins, A.S., King, R.C., Morley, C.K., Drysdale, R.N., 2017. Constraining the timing of shale detachment faulting: a geochronological approach. Lithosphere 9, 431–440.
Hara, H., Kunii, M., Miyake, Y., Hisada, K., Kamata, Y., Ueno, K., Kon, Y., Kurihara, T., Ueda, H., Assavapatchara, S., Treerotchananon, A., Charoentitirat, T., Charusiri, P., 2017. Sandstone provenance and U-Pb ages of detrital zircons from Permian-Triassic forearc sediments within the Sukhothai Arc, northern Thailand: record of volcanic-arc evolution in response to Paleo-Tethys subduction. J. Asian Earth Sci. 146, 30–55.
Hara, H., Tokiwa, T., Kurihara, T., Charoentitirat, T., Ngamnithiporn, A., Visetnat, K., Tominaga, K., Kamata, Y., Ueno, K., 2018. Permian-Triassic back-arc basin development in response to Paleo-Tethys subduction, Sa Kaeo-Chanthaburi area in Southeastern Thailand. Gondwana Res. 64, 50–66.
Hara, H., Ito, T., Tokiwa, T., Kong, S., Lim, P., 2020. The origin of the Pailin Crystalline Complex in western Cambodia, and back-arc basin development in the Paleo-Tethys Ocean. Gondwana Res. 82, 299–316.
Hara, H., Tokiwa, T., Kurihara, T., Charoentitirat, T., Sardsud, A., 2021. Revisiting the tectonic evolution of the Triassic Palaeo-Tethys convergence zone in northern Thailand inferred from detrital zircon U-Pb ages. Geol. Mag. 158, 905–929.
Horiuchi, Y., Charusiri, P., Hisada, K., 2012. Identification of an anastomosing river system in the Early Cretaceous Khorat Basin, northeastern Thailand, using stratigraphy and paleosols. J. Asian Earth Sci. 62, 62–77.
Jiang, H., Li, W.Q., Zhao, K.D., Zhang, D., Jiang, S.Y., 2021. Middle Triassic diorites from the Loei Fold Belt, NE Thailand: petrogenesis and tectonic implications in the context of Paleotethyan subduction. Lithos 382–383, 105955.
Kamata, Y., Sashida, K., Ueno, K., Hisada, K., Nakornsiri, N., Charusiri, P., 2022. Triassic radiolarian faunas from the Mae Sariang area, northern Thailand and their paleogeographic significance. J. Asian Earth Sci. 20, 491–506.
Kamvong, T., Zaw, K., Meffre, S., Maas, R., Stein, H., Lai, C.K., 2014. Adakites in the Truong Son and Loei fold belts, Thailand and Laos: genesis and implications for geodynamics and metallogeny. Gondwana Res. 26, 165–184.
Kawakami, T., Nakanno, N., HIgashino, F., Hodaka, T., Osanai, Y., Yuhara, M., Charusiri, P., Kamikubo, H., Yonemura, K., Hirata, T., 2014. U–Pb zircon and CHIME monazite dating of granitoids and high-grade metamorphic rocks from the Eastern and Peninsular Thailand — a new report of Early Paleozoic granite. Lithos 200–201, 64–79.
Khamfoo, P., 2022. Taxonomy of the Late Paleozoic corals in limestone conglomerate at Phu Nam Yod fossil site, Southwestern Phetchabun, Thailand. Graduate School of Science and Technology, University of Tsukuba, Japan, p. 65. Unpublished M.S. thesis.
Khaowiset, K., Chanfoo, N., 2009. Geological Map of Changwat Phetchabun (Scale 1:250,000). Department of Mineral Resources, Bangkok.
Kouchi, Y., Orihashi, Y., Obara, H., Fujimoto, T., Haruta, Y., Yamamoto, K., 2015. Zircon U– Pb dating by 213 nm Nd:YAG laser ablation inductively coupled plasma mass spectrometry: optimization of the analytical condition to use NIST

SRM 610 for Pb/U fractionation correction. Chikyukagaku (geochemistry) 49, 1–17. in Japanese with English Abstract.
Lacassin, R., Leloup, H., Trinh, P.T., Tapponnier, P., 1998. Unconformity of red sandstones in northern Vietnam: field evidence for Indosinian orogeny in northern Indochina? Terra Nova 10, 106–111.
Le Bas, M.J., Streckeisen, A.L., 1991. The IUGS systematics of igneous rocks. J. Geol. Soc. London 148, 825–833.
Liu, H., Wang, Y., Cawood, P.A., Fan, W., Cai, Y., Xing, X., 2015. Record of Tethyan ocean closure and Indosinian collision along the Ailaoshan suture zone (SW China). Gondwana Res. 27, 1292–1306.
Liu, H., Wang, Y., Li, Z., Zi, J.W., Huangfu, P., 2018. Geodynamics of the Indosinian orogeny between the South China and Indochina blocks: insights from latest Permian-Triassic granitoids and numerical modeling. Bull. Geol. Soc. Amer. 130, 1289–1306.
Ludwig, K.R., 2012. User's Manual for Isoplot 3.75. Special Publication. No. 5. Berkeley Geochronology Center, Berkeley, CA.
Macdonald, A.S., Barr, S.M., 1984. The Nan River mafic-ultramafic belt, northern Thailand: geochemistry and tectonic significance. Geol. Soc. Malaysia Bull. 17, 209–224.
Martin, J.E., Lauprasert, K., Buffetaut, E., Liard, R., Suttethorn, V., 2014. A large Pholidosaurid in the Phu Kradung Formation of North-eastern Thailand. Paleontol. 57, 757–769.
McDonough, W.F., Sun, S., 1995. The composition of the Earth. Chem. Geol. 120, 223–253.
Meesok, A., 2011. Cretaceous. In: Ridd, M.F., Barber, A.J., Crow, M.J. (Eds.), The Geology of Thailand. Geol. Soc, London, pp. 169–184.
Meesok, A., Saengsrichan, W., 2011. Jurassic. In: Ridd, M.F., Barber, A.J., Crow, M.J. (Eds.), The Geology of Thailand. Geol. Soc, London, pp. 151–168.
Meschede, M., 1986. A method of discriminating between different types of mid-ocean ridge basalts and continental tholeiites with the Nb–Zr–Y diagram. Chem. Geol. 56, 207–218.
Metcalfe, I., 2021. Multiple Tethyan ocean basins and orogenic belts in Asia. Gondwana Res. 100, 87–130.
Minezaki, T., Hisada, K., Hara, H., Kamata, Y., 2019. Tectono-stratigraphy of Late Carboniferous to Triassic successions of the Khorat Plateau Basin, Indochina Block, northeastern Thailand: initiation of the Indosinian Orogeny by collision of the Indochina and South China blocks. J. Asian Earth Sci. 170, 208–224.
Miyahigashi, A., 2014. Foraminiferal fauna and sedimentary environment of Carbonate Formations in the Lampang Group of northern Thailand. Fukuoka Univ. Sci. Rep. 44, 109–112. in Japanese.
Morley, C.K., Ampaiwan, P., Thanudamrong, S., Kuenphan, N., Warren, J., 2013. Development of the Khao Khwang Fold and Thrust Belt: implications for the geodynamic setting of Thailand and Cambodia during the Indosinian Orogeny. J. Asian Earth Sci. 62, 705–719.
Morley, C.K., Jitmahantakul, S., Pongwapee, S., Vattanasak, H., 2022. Multiphase deformation of an inverted Permian deepwater rift basin: the Nong Pong Formation, Khao Khwang Fold and Thrust Belt. Thailand. J. Asian Earth Sci. 224, 104979.
Nakano, N., Osanai, Y., Owada, M., Binh, P., Hokada, T., Kaiden, H., Bui, V.T.S., 2021. Evolution of the Indochina block from its formation to amalgamation with Asia: constraints from protoliths in the Kontum Massif. Vietnam. Gondwana Res. 90, 47–62.
Nakornsri, N., 1976. Geological Map of Amphoe Ban Mi. (Sheet ND 47-4, Scale 1:250,000). Department of Mineral Resources, Bangkok.
Nualkhao, P., Takahashi, R., Imai, A., Charusiri, P., 2018. Petrochemistry of granitoids along the Loei Fold Belt, northeastern Thailand. Resour. Geol. 68, 395–424.
Orihashi, Y., Nakai, S., Hirata, T., 2008. U-Pb age determination for seven standard zircons using inductively coupled plasma–mass spectrometry coupled with frequency quintupled Nd-YAG (λ = 213 nm) laser ablation system: comparison with LA–ICP–MS zircon analyses with a NIST glass reference material. Resour. Geol. 58, 101–123.
Panjasawatwong, Y., Zaw, K., Chantaramee, S., Limtrakun, P., Pirarai, K., 2006. Geochemistry and tectonic setting of the Central Loei volcanic rocks, Pak Chom area, Loei, northeastern Thailand. J. Asian Earth Sci. 26, 77–90.
Paungya, N., Singtuen, V., Won-in, K., 2020. The Preliminary geotourism study in Phetchabun Province. Thailand. Geoj. Tour. Geosites 31, 1057–1067.
Pearce, J.A., 2008. Geochemical fingerprinting of oceanic basalts with applications to ophiolite classification and the search for Archean oceanic crust. Lithos 100, 14–48.
Phujareanchaiwon, C., Chenrai, P., Laitrakull, K., 2021. Interpretation and reconstruction of depositional environment and petroleum source rock using outcrop gamma-ray log spectrometry from the Huai Hin Lat Formation. Thailand. Front. Earth Sci. 9, 638862.
Qian, X., Feng, Q., Chonglakmani, C., Monji, D., 2013. Geochemical and geochronological constrains on the Chiang Khong volcanic rocks (northwestern Thailand) and its tectonic implications. Front. Earth Sci. 74, 508–521.
Qian, X., Feng, Q., Yang, W., Wang, Y., Chonglakmani, C., Monji, D., 2015. Arc-like volcanic rocks in NW Laos: geochronological and geochemical constraints and their tectonic implications. J. Asian Earth Sci. 98, 342–357.
Qian, X., Wang, Y., Feng, Q., Zi, J.-W., Zhang, Y., Chonglakmani, C., 2016. Petrogenesis and tectonic implication of the Late Triassic post-collisional volcanic rocks in Chiang Khong, NW Thailand. Lithos 248–251, 418–431.
Qian, X., Wang, Y., Srithai, B., Feng, Q., Zhang, Y., Zi, J.W., He, H., 2017a. Geochronological and geochemical constraints on the intermediate-acid volcanic rocks along the Chiang Khong–Lampang–Tak igneous zone in NW Thailand and their tectonic implications. Gondwana Res. 45, 87–99.
Qian, X., Wang, Y., Feng, Q., Zi, J.W., Zhang, Y., Chonglakmani, C., 2017b. Zircon U-Pb geochronology, and elemental and Sr–Nd–Hf–O isotopic geochemistry of post-collisional rhyolite in the Chiang Khong area, NW Thailand and implications for the melting of juvenile crust. Int. J. Earth Sci. 106, 1375–1389.
Racey, A., Goodall, J.G.S., 2009. Palynology and stratigraphy of the Mesozoic Khorat Group red bed sequences from Thailand. In: Buffetaut, E., Cuny, G., Le Loeuff, J., Suteethorn, V. (Eds.), Late Paleozoic and Mesozoic Ecosystems in SE Asia. Geol. Soc., London, Spec. Pub. 315, 69–83.
Racey, A., Love, M.A., Canham, A.C., Goodall, J.G.S., Polachan, S., Jones, P.D., 1996. Stratigraphy and reservoir potential of the Mesozoic Khorat Group. NE Thailand. J. Petroleum Geol. 19, 5–40.
Racey, A., 2009. Mesozoic red bed sequences from SE Asia and the significance of the Khorat Group of NE Thailand. In: Buffetaut, E., Cuny, G., Le Loeuff, J., Suteethorn, V. (Eds.), Late Paleozoic and Mesozoic Ecosystems in SE Asia. Geol. Soc., London, Spec. Pub. 315, 41–67.
Rossignol, C., Bourquin, S., Hallot, E., Poujol, E., Dabard, M.P., Martini, R., Villeneuve, M., Cornée, J.J., Brayard, A., Roger, F., 2018. The Indosinian orogeny: a perspective from sedimentary archives of north Vietnam. J. Asian Earth Sci. 158, 352–380.
Salam, A., Zaw, K., Meffre, S., McPhie, J., Lai, C.K., 2014. Geochemistry and geochronology of the Chatree epithermal gold–silver deposit: implications for the tectonic setting of the Loei Fold Belt, central Thailand. Gondwana Res. 26, 198–217.
Searle, M.P., Whitehouse, M.J., Robb, L.J., Ghani, A.A., Hutchison, C.S., Sone, M., Ng, S. W.P., Roselee, M.H., Chung, S.L., Oliver, G.J.H., 2012. Tectonic evolution of the Sibumasu−Indochina terrane collision zone in Thailand and Malaysia: constraints from new U−Pb zircon chronology of SE Asian tin granitoids. J. Geol. Soc. London 169, 489–500.
Shervais, J.W., 1982. Ti–V plots and the petrogenesis of modern and ophiolitic lavas. Earth Planet. Sci. Lett. 59, 101–118.
Shi, M., Khin, Z., Liu, S., Xu, B., Meffre, S., Cong, F., Nie, F., Peng, Z., Wu, Z., 2021. Geochronology and petrogenesis of Carboniferous and Triassic volcanic rocks in NW Laos: implications for the tectonic evolution of the Loei Fold Belt. J. Asian Earth Sci. 208, 104661.
Simpson, A., Glorie, S., Morley, C.K., Roberts, N.M.W., Gillespie, J., Lee, J.K., 2021. In-situ calcite U-Pb geochronology of hydrothermal veins in Thailand: new constraints on Indosinian and Cenozoic deformation. J. Asian Earth Sci. 206, 104649.
Sláma, J., Košler, J., Condon, D.J., Crowley, J.L., Gerdes, A., Hanchar, J.M., Horstwood, M.S.A., Morris, G.A., Nasdala, L., Norberg, N., Schaltegger, U., Schoene, B., Tubrett, M.N., Whitehouse, M.J., 2008. Plešovice zircon – a new natural reference material for U-Pb and Hf isotope microanalysis. Chem. Geol. 249, 1–35.
Sone, M., Metcalfe, I., 2008. Parallel Tethyan sutures in mainland Southeast Asia: new insights for Palaeo-Tethys closure and implications for the Indosinian orogeny. C. r. Geosci. 340, 166–179.
Srichan, M., 2019. Petrogenesis of Jurassic volcanic rocks in Phayao Province, Thailand. Unpublished M.S. In: Thesis, Graduate School. Chiang Mai University, Thailand, p. 237p.
Srichan, W., Crawford, A.J., Berry, R.F., 2009. Geochemistry and geochronology of Late Triassic volcanic rocks in the Chiang Khong region, northern Thailand. Island Arc 18, 32–51.
Srinak, N., Hisada, K., Kamata, Y., Charusiri, P., 2007. Stratigraphy of the Mae Sariang Group of northwestern Thailand: implication for paleoenvironments and tectonic setting. Nat. Hist. J. Chulalongkorn Univ. 7, 87–108.
Sun, S.S., McDonough, W.F., 1989. Chemical and isotopic systematics of oceanic basalts: implications for mantle composition and processes. In: Saunders, A.D., Norry, M.J. (Eds.), Magmatism in Ocean Basins. Geol. Soc., London, Spec. Pub. 42, pp. 313–345.
Tong, H., Naksri, W., Buffetaut, E., Suttethorn, S., Suteethorn, V., Chantasit, P., Caude, J., 2014. *Kalasinemys*, a new xinjiangchelyid turtle from the Late Jurassic of NE Thailand. Geol. Mag. 156, 1645–1656.
Tran, T.V., Faure, M., Nguyen, V.V., Bui, H.H., Fyhn, M., Nguyen, T.Q., Lepvrier, C., Thomsen, T.B., Tani, K., Charusiri, P., 2020. Neoproterozoic to Early Triassic tectono-stratigraphic evolution of Indochina and adjacent areas: a review with new data. J. Asian Earth Sci. 191, 104231.
Ueno, K., Charoentitirat, T., 2011. Carboniferous and Permian. In: Ridd, M.F., Barber, A.J., Crow, M.J. (Eds.), The Geology of Thailand. Geol. Soc, London, pp. 71–136.
Vermeesch, P., 2012. On the visualization of detrital age distributions. Chem. Geol. 312–313, 190–194.
Vermeesch, P., 2018. IsoplotR: a free and open toolbox for geochronology. Geosci. Front. 9, 1479–1493.
Walder, A.J., Abell, I.D., Platzner, I., Freedman, P.A., 1993. Lead isotope ratio measurement of NIST 610 glass by laser ablation inductively coupled plasma mass spectrometry. Spectrochim. Acta B, 397–402.
Wang, J.G., Hu, X.M., Wu, F.Y., Jansa, L., 2010. Provenance of the Liuqu Conglomerate in southern Tibet: a Paleogene erosional record of the Himalayan-Tibetan orogen. Sed. Geol. 231, 74–84.
Wang, Y., Qian, X., Cawood, P.A., Liu, H., Feng, Q., Zhao, G., Zhang, Y., He, H., Zhang, P., 2018. Closure of the East Paleotethyan Ocean and amalgamation of the Eastern Cimmerian and Southeast Asia continental fragments. Earth-Sci. Rev. 186, 195–230.
Wang, Y., Yang, T., Zhang, Y., Qian, X., Gan, C., Wang, Y., Wang, Y., Senebouttalath, V., 2020. Late Paleozoic back-arc basin in the Indochina block: constraints from the

mafic rocks in the Nan and Luang Prabang tectonic zones. Southeast Asia. J. Asian Earth Sci. 195, 104333.
Wiedenbeck, M., Alle, P., Corfu, F., Griffin, W.L., Meier, M., Oberli, F., von Quadt, A., Roddick, J.C., Spiegel, W., 1995. Three natural zircon standards for U-Th–Pb, Lu–Hf, trace element and REE analyses. Geostand. Geoanaly. Res. 19, 1–23.
Winchester, J.A., Floyd, P.A., 1977. Geochemical discrimination of different magma series and their differentiation products using immobile elements. Chem. Geol. 20, 325–343.
Yang, Y., Zhao, Q., Zhang, D., Charusiri, P., Huang, B., Zhang, P., 2019. Palaeomagnetism of Late Triassic volcanic rocks from the western margin of Khorat Basin, Thailand and its implication for ambiguous inclination shallowing in Mesozoic sediments of Indochina. Geophys. Jour. Int. 219, 897–910.
Zhang, P., Kuang, H., Liu, Y., Meng, Z., Peng, N., Xu, H., 2019. Sedimentary characteristics and provenance of the basal conglomerate of the Late Jurassic-Early Cretaceous Jiaolai Basin, eastern China and their implications for the uplift of the Sulu Orogenic Belt. Int. Geol. Rev. 61, 521–538.